LXR-inducible host E3 ligase IDOL targets a human cytomegalovirus reactivation determinant to promote latency

Luwanika Mlera[1,2], Sebastian Zeltzer[1,2], Donna Collins-McMillen[1,2], Jason C. Buehler[1,2†], Melissa Moy[3], Katie Caviness[2,4§], Louis Cicchini[2,5¶], and Felicia Goodrum[1,2,3,5*]

[1]Department of Immunobiology, University of Arizona, Tucson, AZ 85721, USA

[2]BIO5 Institute, University of Arizona, Tucson, AZ 85721, USA

[3]Graduate Interdisciplinary Program in Cancer Biology, University of Arizona, Tucson, AZ 85721, USA

[4]Graduate Interdisciplinary Program in Genetics, University of Arizona, Tucson, AZ 85721, USA

[5]Department of Molecular and Cellular Biology, University of Arizona, Tucson, AZ 85721, USA

[†]Current address: Imanis Life Sciences, Rochester, MN 55901, USA

[§]Current address: National Biodefense Analysis and Countermeasures Center, Fort Detrick, MD 21702, USA

[¶]Current address: PPD, Inc., 929 N Front St. Wilmington, NC 28401, USA

***Correspondence:** fgoodrum@arizona.edu

Summary

Liver X receptor (LXR) signaling broadly restricts virus replication, however the mechanisms of restriction are poorly defined. Here, we demonstrate that the LXR-inducible cellular E3 ligase IDOL (inducible degrader of low-density lipoprotein receptor, LDLR) restricts replication of the beta-herpesvirus, human cytomegalovirus (HCMV), for the establishment of viral latency. IDOL is highly expressed in undifferentiated hematopoietic cells where HCMV establishes latency, but is sharply downregulated upon differentiation, a stimulus for reactivation. Importantly, IDOL restricts replication by driving the instability of a key viral determinant required for reactivation, the 33-kDa protein encoded by *UL136* (UL136p33). *UL136* encodes multiple proteins that differentially impact latency and reactivation. UL136p33 is targeted for rapid turnover by the proteasome and its stabilization by mutation of lysine residues to arginine results in a failure to quiet replication for latency. We show that IDOL interacts with and targets UL136p33 for turnover, but not the stabilized variant. While induction of IDOL prevents reactivation, IDOL depletion increases viral gene expression in undifferentiated hematopoietic cells. This work establishes the UL136p33-IDOL interaction as a key regulator of the bistable switch between latency and reactivation. It further implicates cholesterol homeostasis as a key determinant of HCMV reactivation whereby UL136p33 acts a sensor at the tipping point between the decision to maintain the latent state or exit latency for reactivation.

Significance

Herpesviruses establish life-long latent infections, which pose an important risk for disease particularly in the immunocompromised. Defining the mechanisms by which herpesviruses establish latency or reactivate from latency is important to controlling disease. Here, we define host cholesterol homeostasis as an important factor in regulating decisions of human cytomegalovirus, a beta-herpesvirus infecting the

56 majority of the population worldwide, to enter or exit the latent infection. The cellular
57 inducible degrader of low-density lipoprotein receptor, IDOL, target a viral determinant
58 of reactivation at for degradation for the establishment of latency. This work defines a
59 pivotal virus-host interaction that allows HCMV to sense changes in host biology to
60 navigate decisions to establish latency or replicate.
61

62 **Introduction**

63 Viral latency, the ability of a virus to persist indefinitely in the infected host, is a hallmark
64 of herpesviruses. Latency is defined as a non-replicative state punctuated by sporadic
65 reactivation events where the virus replicates productively for transmission. Human
66 cytomegalovirus (HCMV) is a beta-herpesvirus that establishes latent infection in
67 hematopoietic progenitor cells (HPCs) and cells of the myeloid lineage (1). Reactivation
68 of HCMV from latency in the immunocompromised can result in life-threatening disease
69 and is a particularly important risk factor in the context of stem cell and solid organ
70 transplantation. The molecular mechanisms by which HCMV senses changes in the host
71 to make decisions to maintain latency or reactivate from latency is important in developing
72 novel strategies to control viral reactivation and subsequent CMV disease.
73

74 Latency is a complex multifactorial phenomenon dependent on viral determinants, host
75 cell intrinsic, innate, and adaptive responses, as well as host cell signaling and chromatin
76 remodeling (2). Current paradigms hold that HCMV reactivation is tightly connected to
77 hematopoietic cell differentiation (3-7) or inflammatory signaling (3, 8-10). However, much
78 remains to be understood about the precise host contributions and key viral factors that

79 navigate the entry into or exit from latency. We and others have defined roles of *UL133-*
80 *138* gene locus encoded within the UL*b*' region of the HCMV genome for latency and
81 reactivation. UL138 is required for latency and functions by regulating cell surface
82 receptor trafficking and signaling (11-14), innate immune responses (15) and also
83 contributes to repression of viral gene expression (16). UL135, by contrast, is required for
84 reactivation from latency, functioning in part by opposing the function of UL138 (17-19).
85 UL136 is expressed as 5 protein isoforms that have differential effects on the
86 establishment of latency or reactivation. The largest, membrane-associated isoforms,
87 UL136p33 (UL136p33) and p26, are required for reactivation, whereas the small, soluble
88 isoforms are required for latency in both *in vitro* and *in vivo* experimental models (20, 21).
89 Importantly, UL136 proteins accumulate with delayed kinetics relative to UL135 and
90 UL138 and maximal accumulation of UL136 products depend on the onset of viral DNA
91 synthesis and/or entry into late phase. Given its kinetics and dependence on viral DNA
92 synthesis for maximal expression, we postulate that UL136 may negotiate checkpoints
93 that function to maintain latency or commitment to reactivation from latency. Identifying
94 host pathways regulating these viral determinants is key to defining the mechanistic basis
95 by which HCMV senses and responds to changes in host biology to maintain latency or
96 reactivate.
97
98 The cellular environment the virus encounters upon infection undoubtedly plays important
99 roles in the establishment of latency with a host of restriction factors prepared to silence
100 the viral genome, as well as a transcriptional milieu that impacts viral gene expression.
101 As an example, we have shown that the cellular transcription factor early growth response

102 factor-1 (EGR-1) drives the expression of UL138 for the establishment of latency (19, 22).
103 As EGR-1 is required to maintain stemness in the bone marrow niche and is highly
104 expressed in undifferentiated hematopoietic cells (23), cells are primed to drive the
105 expression of UL138 for latency upon infection. However, HCMV also regulates EGR-1
106 expression through the differential trafficking and turnover of the host receptor tyrosine
107 kinase, epidermal growth factor receptor (EGFR) upstream of EGR-1 (11, 18, 19) and
108 through direct targeting by microRNAs that promote reactivation (22). Thus, HCMV has
109 evolved to manipulate and utilized host pathways to regulate its gene expression,
110 hardwiring infection into host signaling pathways. With regards to reactivation, activation
111 of the major immediate early (MIE) transcriptional unit, encoding the major transactivators
112 for viral replication, is highly dependent on host transcription factors in myeloid cells (24).
113 Host transcription factors CREB, FOXO3a and AP-1 are downstream of major signaling
114 pathways, including Src, PI3K/Akt, and MEK/ERK, and are important for re-expression of
115 MIE genes (25-27). Further, UL7 encodes a ligand that binds the cellular Fms-like tyrosine
116 kinase 3 receptor (Flt-3R) that when secreted upon reactivation activates PI3K/AKT and
117 MAPK signaling to prevent cell death and stimulate differentiation for reactivation (28, 29).
118 Through its co-evolution with the human host, the biology of HCMV infection has become
119 tightly intertwined with the biology its host, which reflects the complex mechanisms the
120 virus has evolved to “sense” and “respond” to changes in the cellular environment to
121 navigate “decisions" to maintain latency or reactivate from latency.
122
123 Here we demonstrate that the largest isoform of UL136, UL136p33, is targeted for rapid
124 turnover relative to other UL136 protein isoforms and that its instability ($t_{1/2}$~1 h) is

important to the establishment of latency. We identified the LXR-inducible degrader of low-density lipoprotein receptor (LDLR) IDOL (also known as myosin regulatory light chain interacting protein or MYLIP), as the host E3 ligase that targets UL136p33 for turnover. IDOL expression is induced by oxysterol activation of the liver X receptor (LXR) (30) and is regulated through hematopoietic differentiation (31, 32). In addition to LDLR, IDOL also targets VLDLR and ApoER-2 and, therefore, is an important homeostatic regulator of intracellular cholesterol (30, 33-35). The targeting of UL136p33 by IDOL suggests that the virus has evolved to be responsive to changes in cellular cholesterol in its commitment to reactivation. A model emerges whereby high levels of IDOL maintains low levels of UL136p33 for the establishment of latency, and the downregulation of IDOL by differentiation results in the accumulation of UL136p33 to drive reactivation. Indeed, induction of IDOL results in increased turnover of UL136p33 and prevents reactivation of HCMV from latency, whereas depletion of IDOL increases viral gene expression in hematopoietic cells. Our findings define UL133p33 is a “sensor” of metabolic changes in the cellular environment that allows the virus to make “decisions” to maintain latency or to reactivate.

Results

UL136p33 is unstable and is targeted for proteasomal degradation

UL136 is expressed as at least 5 co-terminal protein isoforms (Fig. 1A). These isoforms are encoded by transcripts with unique 5’ ends and have distinct roles in viral latency and reactivation (20, 21). The largest of these isoforms is a 33 kDa protein (UL136p33) that is required for replication in endothelial cells as well as reactivation from latency in CD34+

148 HPCs and in humanized mice (20). Inversely, the two small isoforms p23 and p19
149 suppress replication in endothelial cells and promote latency in CD34+ HPCs and
150 humanized mice (21). The diametric nature of the UL136 system presupposes additional
151 levels of control to coordinate and commit to one infection program over another, thereby
152 allowing for either optimal replication/reactivation or robust latency. The UL136 isoforms,
153 and particularly the full-length isoform UL136p33, are uniquely labile and sensitive to
154 mechanical lysis while being processed (21). Based on this, we hypothesized that the
155 concentration of some UL136 isoforms is regulated by increased proteolysis, and that the
156 instability of UL136p33 may be important to establishing or maintaining latency.
157
158 To explore the possibility that UL136 isoforms have different stabilities, we analyzed the
159 levels of UL136 isoforms in infected fibroblasts treated with cycloheximide (CHX) to halt
160 protein synthesis. Cycloheximide treatment resulted in a striking loss of UL136p33, p25,
161 and p23, but not p26 or p19 (Fig. 1B, left panel). These results indicated differential
162 stability whereby UL136p33, p25, and p23 may be subject to more rapid turnover, while
163 other UL136 isoforms are relatively stable. Proteasome inhibition robustly rescued
164 UL136p33, p25, and p23 isoforms (Fig. 1B, right panel). Inhibition of the lysosome with
165 NH_4Cl had no effect on rescue of any of the UL136 isoforms; however, inhibition of both
166 the lysosome and proteasome showed a somewhat additive effect. Together, these
167 results indicate that the rapid turnover of UL136p33, p25, and p23 is regulated by the
168 proteasome.
169

170 To establish the kinetics of isoform turnover, we analyzed the decay of UL136 isoforms
171 in fibroblasts infected with TB40/E-*UL136*$_{myc}$ and treated with CHX at peak UL136 isoform
172 expression (Fig 1C). UL136p33 decayed with a half-life of 1 h ($t_{1/2}$=1 h) and p25 exhibited
173 a $t_{1/2}$=3 h, while all other isoforms were stable over the 6 h time course (Fig 1D). Because
174 p23 accumulates to very low levels, the decay of this protein is difficult to determine. The
175 rapid decay of UL136p33 relative to the other isoforms, as well as its significance in
176 HCMV reactivation prompted us to focus on determining the factor(s) contributing to its
177 instability.
178

179 **Lysine to arginine mutations stabilize UL136p33**

180 UL136 has four lysine (K) residues (denoted by red lines in Fig. 1A), three of which lie
181 upstream of the transmembrane domain (TMD) and are specific to UL136p33. To
182 determine if the turnover of UL136p33 was regulated by ubiquitin-mediated proteolysis,
183 we substituted all lysine residues for arginine (R) through site-directed mutagenesis in an
184 expression vector encoding UL136p33 to generate *UL136p33*$_{myc}$*ΔK→R*. The p33$_{\Delta K \rightarrow R}$
185 mutant had a $t_{1/2}$=5 h, compared to ~1 h for UL136p33 following CHX treatment (Fig. 2A).
186 This observation, together with the stabilization of UL136p33 by proteasomal inhibition
187 (Fig. 1B), suggests that UL136p33 turnover is regulated by ubiquitin-mediated
188 proteasomal decay. Further, the rapid turnover of exogenously expressed UL136p33 (Fig.
189 2A, left panel) indicates that UL136p33's degradation is not dependent on virus or virus-
190 induced factors.
191

192 To determine the importance of UL136p33 instability in infection, we introduced the lysine
193 to arginine mutations into the *UL136*$_{myc}$ gene within the bacterial artificial chromosome
194 clone of TB40/E (*UL136*$_{myc}$*ΔK→R*). To test if the mutations translated to increased
195 UL136p33 stability in infection, we measured the relative rates of decay in fibroblasts
196 infected with either the parental *UL136*$_{\mathrm{myc}}$ or *UL136*$_{myc}$*ΔK→R* virus and treated with CHX.
197 p33$_{\Delta K \rightarrow R}$ was stabilized during infection relative to wild type UL136p33 (Fig. 2B).
198 Interestingly, we stabilization of UL136p33 diminished levels of UL136 isoforms p26, p25,
199 and p23.
200
201 We then performed multistep growth curves on fibroblasts infected with *UL136*$_{myc}$ or
202 *UL136*$_{myc}$*ΔK→R* to analyze the impact of stabilizing UL136p33 on virus replication. No
203 change in the kinetics or yield of viral growth was observed during the productive infection
204 in fibroblasts when UL136p33 is stabilized relative to the WT infection (Fig. 2C). This was
205 not surprising since the UL136p33 isoform, while important for replication in endothelial
206 cells and CD34+ HPCs, is dispensable for replication in fibroblasts (20, 21). In summary,
207 UL136p33 instability is the result of lysine-dependent, proteasomal degradation and
208 mutating lysine residues to arginine in *UL136* stabilizes the protein with no effect on virus
209 replication in fibroblasts.
210
211 Since UL136p33 is required for reactivation from latency in CD34+ HPCs (20), we
212 hypothesized that the instability of UL136p33 allows for a tunable concentration gradient
213 which is critical for establishing and maintaining latency. To test this hypothesis, we
214 performed a latency assay in primary human CD34+ HPCs infected with the parental

215 *UL136*$_{\text{myc}}$ or *UL136*$_{myc}$*ΔK→R* viruses. *UL136*$_{myc}$-infected CD34+ HPCs generated >2-fold
216 frequencies of infectious centers following reactivation compared to the pre-reactivation
217 control (Fig. 2D). However, the pre- and post-reactivation frequencies of infectious
218 centers were not different in the *UL136*$_{myc}$*ΔK→R* infection and were almost two-fold above
219 *UL136*$_{\text{myc}}$ pre-reactivation. These results indicate that HCMV replication in CD34+ HPCs
220 is not quieted when UL136p33 is stabilized, and that this virus does not establish a latent
221 infection. As is the case with many viral proteins, UL136 isoforms, even with a myc
222 epitope tag, are not expressed to detectable levels in hematopoietic cells, and we have
223 been unsuccessful in generating antibodies to UL136 isoforms. Nevertheless, the
224 *UL136*$_{myc}$*ΔK→R* infection phenotype is consistent with lower concentrations of UL136p33
225 being important for the establishment of HCMV latency and the accumulation of
226 UL136p33 beyond a critical threshold for commitment to reactivation.
227

228 **The host E3 ligase IDOL targets UL136p33 for proteasomal degradation**

229 Ubiquitination of cargo by E3 ligases is an important step in targeting a protein for
230 proteasomal degradation (36, 37). Because UL136p33 is rapidly turned over by the
231 proteasome even in the absence of infection and the K→R mutations stabilized
232 UL136p33, we hypothesized that a host E3 ligase targets UL136p33 for turnover. We
233 identified UL136 interacting proteins by a yeast two-hybrid screen (Y2H) using the C-
234 terminal region of UL136 (amino acids 141-240) as bait. Intriguingly, we identified the host
235 E3 ligase IDOL (**i**nducible **d**egrader **o**f **l**ow-density lipoprotein receptor), also known as
236 MYLIP, as a candidate host interactor of UL136 (Supporting information, SI Table 1).
237 IDOL induces the degradation of the low-density lipoprotein receptor family members

238 LDLR, VLDLR and ApoER-2 (34, 35). The degradation of these receptors is a
239 physiological response to increased cholesterol, which is modified to oxysterols that
240 activate the liver-X-receptor (LXR) transcription factor to induce *IDOL* expression (35, 38,
241 39).
242
243 To determine if IDOL targets UL136p33, we analyzed the ability of IDOL to interact with
244 and impact UL136p33 levels. We validated the interaction between IDOL and UL136p33
245 by immunoprecipitating (IP) UL136p33-IDOL complexes from cells transiently
246 overexpressing myc-tagged UL136p33 or HA-tagged IDOL. Transient overexpression is
247 necessary due to the lack of an antibody to detect endogenous IDOL. Pulldown of $p33_{myc}$
248 coprecipitated IDOL-HA (Fig. 3A). The reciprocal IP also pulled down the UL136p33-IDOL
249 complex, confirming the interaction between UL136p33 and IDOL. Further, analysis
250 indicated that co-expression of IDOL with UL136p33 resulted in a 60% reduction in
251 UL136p33 levels compared to when UL136p33 was co-expressed with an empty vector
252 (Fig. 3B left panel and Fig. 3C), consistent with IDOL driving UL136p33 turnover. By
253 contrast, $p33_{\Delta K \rightarrow R}$ levels were not affected by IDOL co-expression (Fig. 3B, right panel
254 and Fig. C), in agreement with the hypothesis that ubiquitination on lysine residues is
255 required for UL136p33 turnover via the proteasome (Fig. 1). Taken together, IDOL
256 functions as an E3 ligase that targets UL136p33 for proteasomal degradation.
257
258 We next induced endogenous IDOL expression with an LXR agonist GW3965 or LXR-
259 independent agonist HBX41-108 in cells transiently expressing UL136p33 or $p33_{\Delta K \rightarrow R}$.
260 Because endogenous IDOL cannot be detected by western blot using available

261 antibodies (33, 40, 41), the induction of IDOL was verified by the loss of its target ApoER-
262 2 (Fig. 3D). Induction of IDOL by both GW3965 and HBX41-108 resulted in the
263 degradation of UL136p33 (Fig. 3D, top 3 blots), but not $p33_{\Delta K \rightarrow R}$ (Fig. 3D, bottom 3 blots).
264 These results further confirm that endogenous IDOL targets UL136p33 for degradation.
265
266 The Y2H bait was composed of the C-terminal region of UL136 spanning amino acids
267 141-240 downstream of the predicted TMD. These residues are shared by all the UL136
268 isoforms (Fig. 1A). Further, our data indicated that p25 and p23 proteins are also labile
269 following CHX treatment and these smaller isoforms could be rescued, like UL136p33, by
270 inhibiting the proteasome (Fig. 1B, right panel). The p25 and p23 isoforms have a single
271 lysine which is located downstream of the TMD in the full length UL136 isoform (Fig. 1A).
272 Transient co-expression of IDOL with either p25 or p23 did not lead to any notable
273 turnover of these proteins (SI Fig. 1A-C). These data collectively led us to conclude that
274 IDOL specifically targets UL136p33 for turnover, and it does not mediate the degradation
275 of p25 and p23. The mechanism by which p25 and p23 are turned over remains to be
276 elucidated.
277
278 To further define the specificity of IDOL-mediated turnover of UL136p33, we co-
279 expressed UL136p33 with another E3 ligase, Cbl. Cbl targets tyrosine kinase receptors,
280 such as EGFR, for ubiquitination and subsequent degradation by the lysosome (42).
281 Levels of UL136p33 were unaffected by co-expression with Cbl (SI Fig. 1D-E), indicating
282 specificity of IDOL for proteasomal turnover of UL136p33.
283

284 **IDOL impacts UL136p33 protein levels in HCMV-infected primary fibroblasts**

285 In the context of a productive infection in fibroblasts, we found that infection with either
286 the parental *UL136*$_{myc}$ or a *UL136*$_{myc}$*ΔK→R* induced *IDOL* transcripts by at least 5-fold
287 compared to mock-infection by reverse transcriptase, quantitative PCR (RT-qPCR), (SI
288 Fig. 2A). *IDOL* transcript upregulation was sustained over time during infection and
289 peaked at close to 10-fold by 3 dpi. No changes in *IDOL* transcript levels were detected
290 in mock controls over the same time-course. Because *IDOL* induction is a consequence
291 of increased cellular cholesterol, we measured cholesterol content in infected cells to
292 correlate it to the upregulation of *IDOL* transcripts. Using this approach, we noted that
293 HCMV increased cholesterol concentration by at least 29% from 1 dpi (SI Fig. 1B),
294 consistent with previous findings on HCMV-modulation of lipid biosynthesis (43-48).
295 Taken together, infection in fibroblasts upregulates expression levels of IDOL transcripts,
296 which is correlated with increased intracellular cholesterol levels.

297

298 To address the effect of HCMV-mediated induction of IDOL on UL136p33 levels in a
299 productive infection, we again induced IDOL expression with the LXR agonist GW3965
300 or HBX41-108 in TB40/E-*UL136*$_{myc}$- or -*UL136*$_{myc}$ΔK→R-infected fibroblasts. IDOL
301 induction resulted in a 50% reduction in the levels of UL136p33 but did not significantly
302 affect p33$_{ΔK→R}$ levels (SI Fig. 2C and D). Diminished levels of smaller UL136 isoforms are
303 again apparent in the *UL136*$_{myc}$ΔK→R infection. We next disrupted *IDOL* expression in
304 fibroblasts to answer the question whether IDOL depletion would rescue UL136p33
305 turnover. CRISPR-mediated knockout (KO) of *IDOL* using guide RNAs to disrupt all the
306 isoforms of IDOL was validated by Sanger sequencing and increased ApoER-2 as a proxy

307 for IDOL KO (SI Fig. 2E). Further, CRISPR KO of *IDOL* had no effect on HDAC1, a
308 potential off-target hit when knocking out *IDOL*. In fibroblasts depleted of IDOL, UL136p33
309 levels increased at 2 and 3 dpi compared to luciferase KO controls (SI Fig. 2F and G).
310 Further, IE2 levels were also significantly increased in the $UL136_{myc}$ virus infection of
311 IDOL KO cells (SI Fig. 2H), consistent with a role for UL136p33 in promoting virus
312 replication. As expected, depletion of IDOL had no significant impact on $p33_{\Delta K \rightarrow R}$ and
313 differences in IE2 expression levels were not evident in the context of a $UL136_{myc}\Delta K \rightarrow R$
314 infection (SI Fig 2 G-H). Together, these results indicate that IDOL regulates UL136p33
315 concentration, which indirectly impacts IE expression in the context of infection.
316

317 **Induction of IDOL in CD34+ HPCs restricts HCMV reactivation**

318 To define the role of IDOL on reactivation from latency in primary CD34+ HPCs, we
319 induced IDOL expression with the LXR agonist GW3965 in combination with a
320 reactivation stimulus. *IDOL* induction was validated by increased IDOL transcripts in
321 GW3965-treated cells compared to DMSO-treated cells (Fig. 4A). Induction of IDOL with
322 GW3965 in CD34+ HPCs restricted reactivation from latency relative to the DMSO control
323 (Fig. 4B), consistent with a requirement for accumulation of UL136p33 for reactivation.
324 Strikingly, reactivation of the $UL136_{myc}\Delta K \rightarrow R$ was not restricted by GW3965-induction of
325 IDOL. Taken together, these results support the hypothesis that UL136p33 stability is
326 required for reactivation from latency and that induction of IDOL at reactivation
327 suppresses UL136p33 from accumulating to levels sufficient for reactivation.
328

329 **IDOL is regulated by differentiation in THP-1 monocytes to suppress viral protein**
330 **expression**

331 We next wanted to understand how IDOL was regulated in hematopoietic cells and its
332 impact on CMV gene expression and latency in hematopoietic cells. THP-1 monocytes
333 are a model cell line in which HCMV establishes latency in undifferentiated cells, and a
334 re-expression of viral genes for reactivation can be stimulated by differentiating the cells
335 into macrophages with a phorbol ester, tetradecanoylphorbol acetate (TPA) (49-54).
336 Because dynamic gene expression changes are associated with monocyte-to-
337 macrophage differentiation (31, 55, 56), we hypothesized that IDOL expression in THP-1
338 cells may be dictated by the differentiation state of the cell. Indeed, we found that *IDOL*
339 mRNA was highly expressed in undifferentiated THP-1 monocytes prior to infection, but
340 were sharply downregulated upon THP-1 cell differentiation (Fig. 5A). Further, while no
341 significant differences in *IDOL* expression were observed between uninfected cells and a
342 $UL136_{myc}$ infection, $UL136_{myc}\Delta K\rightarrow R$ infection significantly downregulated *IDOL*
343 expression in the undifferentiated, latent phase (Fig. 5A), suggesting that UL136p33
344 levels may feedback to impact IDOL expression in a cell type-dependent manner.
345

346 To determine how IDOL impacts HCMV infection in hematopoietic cells, we knocked out
347 IDOL in THP-1 cells. The knockdown was validated using an ELISA assay for the
348 detection of IDOL protein (Fig. 5B). Further, *IDOL* KO had no off-target effects on HDAC1
349 (Fig. 5C). Given the challenges of detecting UL136 isoforms, particularly in hematopoietic
350 cells, we examined UL135 and IE gene expression as proxies for determining the effect
351 of *IDOL* KO in infected THP-1 cells. UL135 and IE proteins are detected early during

352 infection in THP-1 cells but diminish as the virus establishes latency between 3 and 5 dpi
353 (Fig. 5 D-E, upper panel) (49). *IDOL* KO resulted in an increased burst in the expression
354 of IEs and UL135 at 1 dpi relative to control *Luc* KO cells, consistent with increased
355 UL136p33 levels as observed in fibroblasts. Intriguingly, the burst was relatively quieted
356 by 5 dpi, suggesting that other inherent cellular factors may impact HCMV protein
357 expression during latent infection. In a $UL136_{myc}\Delta K\rightarrow R$ there were no apparent
358 differences in IEs or UL135 expression due to the KO of IDOL, as expected (Fig. 5D-E,
359 lower panels). These results indicate that IDOL expression in undifferentiated THP-1 cells
360 suppresses viral protein expression to drive a latent program, consistent with its role in
361 maintaining low levels of UL136p33.
362

363 ***De novo* cholesterol biosynthesis is required for HCMV reactivation from latency**

364 Because LXR-mediated induction of IDOL is linked to cholesterol metabolism, we asked
365 if there was a direct connection between host cholesterol metabolism and HCMV latency.
366 To address this question, we measured cholesterol concentration in infected THP-1 cells.
367 In contrast to infection in fibroblasts (SI Fig. 1B), the non-replicative infection in THP-1
368 cells did not induce cholesterol synthesis (Fig. 6A). A 14% increase was observed at 1
369 dpi, but it was not statistically significant and was not sustained. However, differentiation
370 with TPA significantly increased cholesterol concentrations relative to undifferentiated
371 cells, yet again there was no significant difference between mock- and HCMV-infected
372 cells. These results are consistent with increases in cholesterol observed with
373 differentiation and suggest that HCMV has a limited ability to alter cholesterol levels in
374 hematopoietic cells.

375

376 Next, we hypothesized that inhibition of *de novo* cholesterol biosynthesis at differentiation
377 would suppress reactivation. To test this hypothesis, we used the statin, pravastatin
378 (PRV), to block *de novo* cholesterol biosynthesis by inhibiting the rate limiting enzyme
379 HMG-CoA reductase. PRV inhibition of *de novo* cholesterol biosynthesis was validated
380 by measuring relative *SREBP2* transcripts (Fig. 6B), which are upregulated in response
381 to cholesterol depletion (57-59). HMGcO-A reductase converts HMG-CoA tp mevalonate
382 (MEV) for isoprenoid synthesis (60-62). Providing mevalonate (MEV), the product of
383 HMG-CoA reductase, will rescue the statin-induced depletion of cholesterol (63, 64). As
384 such, we find that feeding cells MEV rescued the induction of SREBP2. Consistent with
385 the requirement for cholesterol for HCMV replication. PRV restricted the expression of
386 both IE1 and IE2 in THP-1 cells infected with HCMV and differentiated to reactivate (Fig.
387 6C). Consistent with this finding, another statin, Simvastatin, also inhibited IE1 and IE2
388 gene expression (SI Fig. 2). However, we were suprisingly unable to rescue IE1 and IE2
389 gene expression with MEV treatment. These results support the hypothesis that *de novo*
390 cholesterol biosynthesis is required for reactivation from latency, but raises the question
391 as to whether cholesterol itself is the important factor driving replication.

392

393 It was recently reported that statins attenuate poly:(IC)-induced IFN-β expression via
394 inhibition of JAK/STAT signaling in mouse macrophages (65). Moreover, MEV prevented
395 the statin-mediated suppression of IFN-β. We explored this by analyzing IFN-β
396 expression in THP-1 cells treated with PRV with or without MEV. Consistent with Koike
397 et al. (66), PRV treatment trended towards suppressing *IFN-β1* transcripts relative to TPA

398 treatment alone (Fig. 6D). Further, the addition of MEV resulted in a significant
399 upregulation *IFN-β1*. Because HCMV is sensitive to IFN (67-69), we reasoned that IFN-
400 β stimulated by the combined effect of PRV and MEV was preventing our attempt to
401 rescue reactivation. To determine if MEV induced an IFN-dependent block to HCMV gene
402 expression, we inhibited IFN signaling using the Jak inhibitor, ruxolitinib (Rux) (70), which
403 reduced levels of active phosphorylated signal transducer and activator of transcription
404 (pSTAT1) in differentiated THP-1 cells (Fig. 6E). Consistent with the possibility that MEV-
405 mediated induction of *IFN-β1* restricted HCMV gene expression, RUX treatment rescued
406 IE1 and IE2 gene expression in infected THP-1 cells stimulated to differentiation in the
407 context of PRV/MEV treatment resulted in robust rescue of IE transcript expression (Fig.
408 6F). Taken together, these results indicate that *de novo* cholesterol biosynthesis is
409 required for reactivation of HCMV from latency.
410

411 **Discussion**

412 Latent viruses require mechanisms to sense the cellular environment, filter noise and
413 respond to host cues to make solid decisions to maintain a quiescent latent state or to
414 reactivate replication (1). While the decision to enter or exit latency is often depicted as a
415 simple binary on/off switch, the reality is that a number of thresholds must be cleared for
416 the commitment to productive reactivation. Developing strategies to control entry into or
417 exit from CMV latency and ultimately control CMV disease rests upon identifying the virus-
418 host interactions that govern the decisions around latency and reactivation. Here we
419 demonstrate the existence of an unstable viral determinant of reactivation, UL136p33.
420 We demonstrate that its instability is dependent upon a host E3 ligase, IDOL, which is

421 regulated by hematopoietic differentiation. Our results support a model whereby
422 UL136p33 is maintained at low levels for the establishment of latency because IDOL
423 levels are high (Fig. 7). Upon differentiation, IDOL levels fall allowing UL136p33 levels to
424 rise, which facilitates HCMV crossing at least one threshold towards reactivation.
425 UL135p33 levels are further ensured by the onset of viral DNA synthesis and entry into
426 late phase (21). These findings define novel virus-host interactions that govern entry into
427 and exit from latency. Moreover, these findings suggest that by utilizing IDOL to regulate
428 levels of a critical determinant for reactivation, the virus has evolved to hardwire this
429 decision into the regulation of intracellular cholesterol, which ultimately controls IDOL
430 levels.
431
432 *IDOL* is transcriptionally upregulated by excess cholesterol derivatives (oxysterols) that
433 are sensed by LXR (35, 71-74). Indeed, HCMV infection remodels the cellular lipid
434 metabolic landscape by upregulating *de novo* cholesterol biosynthesis during a
435 productive infection (44, 47, 48). It is, therefore, expected that HCMV infection would
436 induce IDOL expression. IDOL recognizes a conserved motif WxxKNxxSI/MxF within the
437 cytoplasmic tail of its targets (ApoER-2, LDLR and VLDLR), to mediate ubiquitination for
438 lysosomal degradation (30, 34, 35, 75). Canonical IDOL targets reside at the plasma
439 membrane and are typically internalized via the endocytosis and trafficked to the
440 lysosome (75). By contrast, UL136p33 is predominantly Golgi-associated (21), lacks a
441 WxxKNxxSI/MxF motif and, is degraded via the proteasome (Fig. 1B). Thus, differences
442 in localization and trafficking pathways between natural IDOL targets and UL136p33 may
443 differentially direct the degradation pathway.

444

445 Activation of LXR in human foreskin fibroblasts with GW3965 prior to HCMV infection was
446 reportedly shown to depresses expression levels of viral proteins, such as IE2, pp28,
447 pp65 and gB (76). GW3965 treatment is also reported to induce IFN-γ (77), a cytokine
448 which directly inhibits IE1/2 mRNA expression (78). These findings might suggest that
449 possibility that the effects of LXR agonists on UL136p33 levels are due to a global
450 repression of viral gene expression. However, our results argue against this scenario.
451 First, we observed no effect on IE gene expression at 2 dpi in infected fibroblasts treated
452 with GW3965 or HBX41-108 (Fig. S1C), consistent with the attenuation of IFN-γ at later
453 times (79). Second, specific depletion of *IDOL* increases UL136p33, consistent with
454 IDOL-specific effects on UL136p33 levels.

455

456 Regulation of IDOL is, in part, controlled by the cell niche. RNA sequencing to classify the
457 tissue-specific expression of genes across a representative set of all major human organs
458 and tissues revealed that IDOL is highly upregulated in the bone marrow (BM), where
459 CD34+ HPCs and monocytes and are generated, at 31 RPKM (reads per kilobase per
460 million mapped reads) (80). The level of IDOL expression in the BM is only second to the
461 placenta. High expression of IDOL in undifferentiated progenitor cells suggests they are
462 intolerant of high cholesterol levels. Consistent with this, undifferentiated THP-1
463 monocytes express significantly higher levels of cholesterol efflux genes, such as CES1,
464 and express significantly lower levels of influx genes (81). By contrast, THP-1 monocyte-
465 derived macrophages upregulate cholesterol influx genes, such as scavenger receptor
466 A1 (SR-A1) and CD36 to become lipid-loaded macrophages or foam cells. Further, statin

467 treatment to lower cholesterol reduces CD34+ HPC populations in the circulation and
468 high cholesterol promotes CD34+ HPC proliferation, myelopoiesis as well as monocyte
469 and granulocytic differentiation (82-84). While carefully designed studies are required to
470 understand how statins specifically affect HCMV latency and/or reactivation, these
471 findings suggest the possibility that untreated hypercholesterolemia might lead to
472 increased hematopoietic differentiation and a higher frequency of HCMV reactivation
473 events, whereas statin treatments may restrict HCMV reactivation and replication. Given
474 the role demonstrated here for IDOL in the regulation of cholesterol and UL136p33
475 expression, the high levels of IDOL expression and the relatively low levels of cholesterol
476 make progenitor cells an ideal environment for HCMV latency in which UL136p33 is
477 suppressed by rapid turnover.
478
479 The LXR axis is important for the biology of other herpesviruses. A recent report
480 demonstrates that the alpha herpesvirus pseudorabies virus (PRV), etiologic agent of the
481 economically important Aujeszky's disease, has evolved to inhibit LXR at both
482 transcription and protein levels (85). Using an inverse LXR agonist SR9243, Wang and
483 colleagues showed that inhibiting LXR increased PRV replication, whereas 3 different
484 LXR agonists and the oxysterol 22R-hydroxycholesterol all inhibited virus replication (85).
485 However, PRV can be rescued from the suppressive effects of an LXR agonist by
486 supplementing with cholesterol (85), consistent with a viral need for cholesterol to
487 replicate. LXR also inhibits the murine gamma herpesvirus MHV68 as it replicates better
488 in *LXR*$^{-/-}$ macrophages and, contrary to PRV, MHV68 infection increases LXRα (86).
489 Importantly, LXRα restricts reactivation of MHV86 in peritoneal cells, but not in

490 splenocytes (87). The cell type-dependent role of LXR signaling for reactivation suggests
491 the possibility that a LXR signaling might control a MHV68 determinant of reactivation in
492 peritoneal cells that is dispensable in splenocytes. Similarly, disruption of or stabilization
493 of UL136p33 did not impact replication in fibroblasts (Fig. 2C) (21), but did impact
494 replication in HPCs and endothelial cells (Fig. 2D) (20). Viral factors encoded by MHV68
495 and regulated by LXR signaling have yet to be determined.
496
497 Apart from herpesviruses, suppresses the replication of other viruses, including Hepatitis
498 C Virus (HCV) (88, 89), human immunodeficiency virus (HIV) (90-92), and Newcastle
499 disease virus (NDV) (93). Intriguingly, activation of LXR signaling suppresses hepatitis C
500 virus (HCV) replication in an IDOL-dependent manner. The suppression of HCV is
501 presumably due to the requirement of LDLR for an entry receptor since once infection is
502 established, IDOL induction does not seem to have an effect on HCV replication (94).
503 However, there are mixed reports on the requirement for LDLR for HCV entry or its
504 specific function in HCV replication (95-97).
505
506 While many host pathways are implicated in the regulation of herpesvirus latency, the
507 interplay between viral determinants and their regulation by host mechanisms to
508 terminate activity is less well appreciated, particularly for HCMV. The expression of HSV-
509 1 ICP0, a critical protein for reactivation and replication, is suppressed by the host
510 neuronal microRNA-138 to facilitate latency (98, 99). Moreover, ICP0 was recently shown
511 to be regulated by the host E3 ligase, TRIM23, which is in turn countered by the HSV-1
512 late protein, $\gamma_1$34.5 (100). While speculative, TRIM23 may moderate ICP0 protein levels

513 to suppress reactivation, where $\gamma_1$34.5 ensures the commitment to replication by blocking
514 TRIM23-mediated turnover of ICP0. Further, the E3 ubiquitin ligase, MDM2, restricts
515 levels of the Kaposi's sarcoma-associated herpesvirus (KSHV) transactivator,
516 RTA/ORF50, acting as pro-viral factor for latency (101). RTA/ORF50 in turn induces
517 degradation of vFLIP through the host Itch E3 ubiquitin ligase to attenuate vFLIP-driven
518 NFκB signaling for reactivation (102, 103). It will be important to determine if UL136p33
519 feedsback to regulate IDOL expression based on the observation that stabilization of
520 UL136p33 represses IDOL expression in undifferentiated THP-1 cells (Fig. 5A). Coopting
521 and regulating host E3 ligases to target viral proteins for latency allows infections to
522 respond quickly (e.g., prior to changes requiring transcription of genes and translation of
523 proteins) to stimuli for reactivation. It will be important to further define the mechanisms
524 by which UL136p33 interacts with host pathways to impact viral gene expression and
525 promote context-dependent replication and reactivation.
526
527 The evolution of viruses to depend on host factor-mediated turnover of critical viral
528 determinants is shared across highly divergent systems. Bacteriophages establish a
529 dormant lysogenic state to cope with their variable and unpredictable environment (104).
530 Bacteriophage λ lysogeny depends on the competition between repressors and activators
531 of gene expression that serve as a gatekeeper for the lytic pathways (105, 106). As a
532 primary example, competitive binding of the lysogeny determinant CI and the immediate
533 early gene Cro at regulatory operator elements puts CI-Cro at the heart of a bistable
534 switch controlling lysogenic-lytic decisions. Another determinant, CII, is expressed with
535 later kinetics and is also critical to the commitment to lysogeny (107, 108). CII promotes

536 expression of CI while it represses expression of the anti-terminator Q, that must
537 accumulate to a threshold to drive lytic gene expression. Critical effectors in
538 bacteriophage lysogeny, such as CI and CII, are susceptible to destruction by host
539 proteases that are induced in response to stresses, such as DNA damage (109, 110). As
540 such, the decision to establish lysogeny depends on the accumulation of lysogenic
541 effectors and is responsive to host determinants regulated by environmental cues.
542 Further, while CI is robust, the expression of CII, like UL136, is sensitive to genome copy
543 number or other fluctuations in the system, providing additional checkpoints in regulating
544 the decision.
545
546 With respect to the system emerging for HCMV, the *UL133-UL138* locus coordinates the
547 expression of multiple genes impacting infection fate decisions. While UL135 and UL138
548 are not known to directly regulate gene expression, their opposing impact on host
549 EGFR/PI3K signaling (11, 17, 19) has parallels to the Cro-CI bistable genetic switch.
550 Further, UL136p33 is expressed with later kinetics than the UL135/UL138 determinants,
551 and its expression is dependent on crossing a threshold of viral DNA synthesis (21). In
552 addition, UL136p33 is remarkably unstable compared to other *UL133-UL138* genes and
553 other UL136 isoforms, and, as we have shown here, its instability is dependent upon a
554 host E3 ligase regulated by differentiation-linked changes in cholesterol homeostasis.
555 Although the UL136p33 protein is undetectable in THP-1 monocytes, KO of *IDOL*
556 increases expression of genes critical for replication (e.g., IEs and UL135). While UL135
557 is critical for overcoming the repressive effects of UL138 for successful reactivation, we
558 assert that the subsequent accumulation of UL136p33 beyond a threshold is also

559 important for commitment to the replicative state (Fig. 7). It will be important to understand
560 the relationship between UL135 and UL136p33 in the commitment to HCMV reactivation
561 since as both are required for reactivation and how other UL136 isoforms, for example
562 the latency-promoting UL136p23/19 isoforms (20), may counter the progression towards
563 reactivation to maintain a latent infection.
564
565 In conclusion, we have identified a host E3 ligase, IDOL, which controls UL136p33
566 concentrations by targeting it for turnover. IDOL is regulated by cell differentiation in a
567 cholesterol-linked manner. UL136p33 concentrations are critical to exit from latency.
568 Thus, HCMV senses changes in the host cell cholesterol environment through UL136p33
569 levels to make decisions to enter or exit latency. It will be important to understand how
570 HCMV infection regulates IDOL levels, potentially through UL136p33 feedback, during
571 latency or replicative states to further influence latent-replication decisions. Further, the
572 LXR-IDOL axis may be a potential target for studies aimed at controlling HCMV
573 reactivation clinically.
574
575 **Methods**
576 **Cells and viruses**
577 Human primary embryonic fibroblasts (MRC-5; ATCC) and human kidney embryonic
578 293T (HEK 293T; ATCC) cells were maintained in Dulbecco's Essential Media (DMEM).
579 The DMEM was supplemented with 10% fetal bovine serum (FBS), 10 mM HEPES, 1 mM
580 sodium pyruvate, 2 mM l-alanyl-glutamine, 0.1 mM nonessential amino acids, 100 U/ml
581 penicillin, and 100 μg/ml streptomycin. CD34+ hematopoietic progenitor cells (HPCs)

582 were isolated from de-identified medical waste following bone marrow isolations from
583 healthy donors for clinical procedures at the Banner-University Medical Center at the
584 University of Arizona (111). THP-1 cells were maintained in RPMI1640 (Gibco)
585 supplemented with 10% FBS, 1 mM sodium pyruvate, 0.1 mM β-mercapto-ethanol
586 (Sigma).
587
588 The wild type TB40E/05 strain expressing GFP as a marker for infection (112) was
589 engineered to fuse the myc epitope tag in frame at the 3' end of *UL136* (*UL136*$_{myc}$ virus)
590 using BAC recombineering as described previously (21). The *UL136*$_{myc}$*ΔK→R* virus was
591 constructed following methods previously described (Caviness 2014). See SI for detailed
592 description of virus recombineering.
593
594 **CRISPR/CAS9-mediated knock out of *IDOL***
595 Guide RNAs (gRNAs) used to knock out IDOL were designed using online gRNA design
596 tools at atum.bio and synthego.com. Sequences of the gRNAs are shown in SI Table 2.
597 The gRNAs were cloned into lentiCRISPR v2 (113). Lentiviruses to deliver the gRNAs
598 were generated by co-transfecting the lentiCRISPR v2 constructs with pDMG.2 and
599 psPAX2 in HEK 293T cells. MRC-5 and THP-1 cells were transduced at a MOI of 3 and
600 10, respectively. Transduced cells were selected with 2 µg/ml puromycin for 2 days.
601 Validation of knock-out was done by blotting for ApoER-2, Sanger sequencing or
602 quantifying levels of IDOL by ELISA. The Synthego gRNA design algorithm
603 (synthego.com) indicates potential off-target genes for the gRNAs and we selected
604 *HDAC1* to evaluate potential off-target effects by western blot analyses.

605

606 **IDOL ELISA**

607 We used a sandwich ELISA assay (Cusabio) to quantify IDOL protein levels in THP-1
608 cells. Cells were washed in cold PBS and resuspended at 10^8 cells/mL followed by
609 freezing at -20 ^{o}C. Following 3 freeze-thaw cycles, IDOL was quantified according to the
610 manufacturer's protocol. Optical densities were determined using a Clariostar plate
611 reader (BMG Labtech) and sample values were interpolated from a standard curve in
612 GraphPad Prism v9.

613

614 **Cholesterol assay**

615 Fibroblasts were seeded at 3 x 10^5 cells per well in 6-well dishes and incubated overnight.
616 Infections were done at a MOI of 1 for 1 h and the inoculum was removed followed by
617 washing cells twice with PBS. Infected cells were incubated in serum-free media and 50
618 000 cells were harvested at appropriate time points. Samples were prepared using a
619 cholesterol Glo bioluminescent assay (Promega) according to the manufacturer's
620 instructions. Relative light unites were measured using a Clariostar Plus plate reader
621 (BMG Labtech) and sample values were extrapolated from a standard curve in GraphPad
622 Prism v9.

623

624 Please see SI for detailed description of materials and methods.

625

626 **Acknowledgements**

627 This study was supported by the National Institutes of Allergy and Infectious Diseases/
628 National Institutes of Health (NIAID/NIH) grants AI079059 and AI131598 to FG. We are
629 grateful for the support of the Flow Cytometry and Human Immune Monitoring Shared
630 Resource, supported through the Cancer Center Support Grant P30 CA023074 awarded
631 to University of Arizona. We appreciate technical assistance from Lincoln Gay. We thank
632 Drs. James Alwine (University of Pennsylvania), Lynn Enquist (Princeton University),
633 Jean Wilson (University of Arizona), and John Purdy (University of Arizona) for critical
634 discussions on this work.

635

636 **References**

637 1. F. Goodrum, "The complex biology of human cytomegalovirus latency and reactivation" in
638 Advances in Virus Research, T. C. M. M. Kielian, M. J. Roossinck, Ed. (Academic Press, 2022), vol.
639 112.
640 2. F. Goodrum, W. Britt, E. S. Mocarski, "Cytomegalovirus" in Fields Virology: DNA Viruses, P. M.
641 Howley, D. M. Knipe, J. L. Cohen, B. A. Damania, Eds. (Wolters Kluwer, 2022), vol. 2, chap. 12.
642 3. G. Hahn, R. Jores, E. S. Mocarski, Cytomegalovirus remains latent in a common precursor of
643 dendritic and myeloid cells. *Proc Natl Acad Sci U S A* **95**, 3937-3942 (1998).
644 4. C.-K. Min *et al.*, The Differentiation of Human Cytomegalovirus Infected-Monocytes Is Required
645 for Viral Replication. **10** (2020).
646 5. M. B. Reeves, P. A. MacAry, P. J. Lehner, J. G. P. Sissons, J. H. Sinclair, Latency, chromatin
647 remodeling, and reactivation of human cytomegalovirus in the dendritic cells of healthy carriers.
648 *Proceedings of the National Academy of Sciences of the United States of America* **102**, 4140 (2005).
649 6. M. B. Reeves, J. H. Sinclair, Circulating dendritic cells isolated from healthy seropositive donors
650 are sites of human cytomegalovirus reactivation in vivo. *J Virol* **87**, 10660-10667 (2013).
651 7. J. Taylor-Wiedeman, J. G. P. Sissons, L. K. Borysiewicz, J. H. Sinclair, Monocytes are a major site of
652 persistence of human cytomegalovirus in peripheral blood mononuclear cells. **72**, 2059-2064
653 (1991).
654 8. E. Forte *et al.*, Tumor Necrosis Factor Alpha Induces Reactivation of Human Cytomegalovirus
655 Independently of Myeloid Cell Differentiation following Posttranscriptional Establishment of
656 Latency. *mBio* **9**, e01560-01518 (2018).
657 9. C. Söderberg-Nauclér, K. N. Fish, J. A. Nelson, Reactivation of Latent Human Cytomegalovirus by
658 Allogeneic Stimulation of Blood Cells from Healthy Donors. *Cell* **91**, 119-126 (1997).
659 10. M. B. Reeves, T. Compton, Inhibition of inflammatory interleukin-6 activity via extracellular signal-
660 regulated kinase-mitogen-activated protein kinase signaling antagonizes human cytomegalovirus
661 reactivation from dendritic cells. *J Virol* **85**, 12750-12758 (2011).
662 11. J. Buehler *et al.*, Opposing Regulation of the EGF Receptor: A Molecular Switch Controlling
663 Cytomegalovirus Latency and Replication. *PLOS Pathogens* **12**, e1005655 (2016).

664 12. M. P. Weekes *et al.*, Latency-Associated Degradation of the MRP1 Drug Transporter During Latent
665 Human Cytomegalovirus Infection. *Science* **340**, 199 (2013).
666 13. V. T. K. Le, M. Trilling, H. Hengel, The Cytomegaloviral Protein pUL138 Acts as Potentiator of Tumor
667 Necrosis Factor (TNF) Receptor 1 Surface Density To Enhance ULb'-
668 Encoded Modulation of TNF-α Signaling. *Journal of Virology* **85**, 13260 (2011).
669 14. C. Montag *et al.*, The Latency-Associated UL138 Gene Product of Human Cytomegalovirus
670 Sensitizes Cells to Tumor Necrosis Factor Alpha (TNF-α) Signaling by Upregulating TNF-α Receptor
671 1 Cell Surface Expression. **85**, 11409-11421 (2011).
672 15. E. R. Albright, C. K. Mickelson, R. F. Kalejta, Human Cytomegalovirus UL138 Protein Inhibits the
673 STING Pathway and Reduces Interferon Beta mRNA Accumulation during Lytic and Latent
674 Infections. *mBio* **12**, e0226721-e0226721 (2021).
675 16. S. H. Lee, E. R. Albright, J.-H. Lee, D. Jacobs, R. F. Kalejta, Cellular defense against latent
676 colonization foiled by human cytomegalovirus UL138 protein. *Sci Adv* **1**, e1501164-e1501164
677 (2015).
678 17. M. Umashankar *et al.*, Antagonistic Determinants Controlling Replicative and Latent States of
679 Human Cytomegalovirus Infection. *Journal of Virology* **88**, 5987 (2014).
680 18. M. A. Rak *et al.*, Human Cytomegalovirus UL135 Interacts with Host Adaptor Proteins To Regulate
681 Epidermal Growth Factor Receptor and Reactivation from Latency. **92**, e00919-00918 (2018).
682 19. J. Buehler *et al.*, Host signaling and EGR1 transcriptional control of human cytomegalovirus
683 replication and latency. *PLOS Pathogens* **15**, e1008037 (2019).
684 20. K. Caviness *et al.*, Complex Interplay of the UL136 Isoforms Balances
685 Cytomegalovirus Replication and Latency. *mBio* **7**, e01986-01915 (2016).
686 21. K. Caviness, L. Cicchini, M. Rak, M. Umashankar, F. Goodrum, Complex expression of the UL136
687 gene of human cytomegalovirus results in multiple protein isoforms with unique roles in
688 replication. *J Virol* **88**, 14412-14425 (2014).
689 22. I. Mikell *et al.*, HCMV miR-US22 down-regulation of EGR-1 regulates CD34+ hematopoietic
690 progenitor cell proliferation and viral reactivation. *PLoS Pathog* **15**, e1007854 (2019).
691 23. I. M. Min *et al.*, The Transcription Factor EGR1 Controls Both the Proliferation and Localization of
692 Hematopoietic Stem Cells. *Cell Stem Cell* **2**, 380-391 (2008).
693 24. D. Collins-McMillen, J. Kamil, N. Moorman, F. Goodrum, Control of Immediate Early Gene
694 Expression for Human Cytomegalovirus Reactivation. *Frontiers in cellular and infection*
695 *microbiology* **10**, 476 (2020).
696 25. B. A. Krishna, A. B. Wass, C. M. O'Connor, Activator protein-1 transactivation of the major
697 immediate early locus is a determinant of cytomegalovirus reactivation from latency. *Proc Natl*
698 *Acad Sci U S A* **117**, 20860-20867 (2020).
699 26. A. E. Hale *et al.*, FOXO transcription factors activate alternative major immediate early promoters
700 to induce human cytomegalovirus reactivation. *Proc Natl Acad Sci U S A* **117**, 18764-18770 (2020).
701 27. V. G. Kew, J. Yuan, J. Meier, M. B. Reeves, Mitogen and stress activated kinases act co-operatively
702 with CREB during the induction of human cytomegalovirus immediate-early gene expression from
703 latency. *PLoS Pathog* **10**, e1004195 (2014).
704 28. L. B. Crawford *et al.*, Human Cytomegalovirus Encodes a Novel FLT3 Receptor Ligand Necessary
705 for Hematopoietic Cell Differentiation and Viral Reactivation. *MBio* **9** (2018).
706 29. M. H. Hancock *et al.*, Human Cytomegalovirus UL7, miR-US5-1, and miR-UL112-3p Inactivation of
707 FOXO3a Protects CD34(+) Hematopoietic Progenitor Cells from Apoptosis. *mSphere* **6** (2021).
708 30. E. Scotti *et al.*, Targeted disruption of the idol gene alters cellular regulation of the low-density
709 lipoprotein receptor by sterols and liver x receptor agonists. *Mol Cell Biol* **31**, 1885-1893 (2011).

710 31. R. G. de Bruin *et al.*, Quaking promotes monocyte differentiation into pro-atherogenic
711 macrophages by controlling pre-mRNA splicing and gene expression. *Nat Commun* **7**, 10846
712 (2016).
713 32. Y. Liu, M. Tingart, S. Lecouturier, J. Li, J. Eschweiler, Identification of co-expression network
714 correlated with different periods of adipogenic and osteogenic differentiation of BMSCs by
715 weighted gene co-expression network analysis (WGCNA). *BMC Genomics* **22**, 254 (2021).
716 33. E. Scotti *et al.*, IDOL stimulates clathrin-independent endocytosis and multivesicular body-
717 mediated lysosomal degradation of the low-density lipoprotein receptor. *Mol Cell Biol* **33**, 1503-
718 1514 (2013).
719 34. C. Hong *et al.*, The E3 ubiquitin ligase IDOL induces the degradation of the low density lipoprotein
720 receptor family members VLDLR and ApoER2. *J Biol Chem* **285**, 19720-19726 (2010).
721 35. N. Zelcer, C. Hong, R. Boyadjian, P. Tontonoz, LXR regulates cholesterol uptake through Idol-
722 dependent ubiquitination of the LDL receptor. *Science* **325**, 100-104 (2009).
723 36. M. H. Glickman, A. Ciechanover, The ubiquitin-proteasome proteolytic pathway: destruction for
724 the sake of construction. *Physiological reviews* **82**, 373-428 (2002).
725 37. C. M. Pickart, Back to the future with ubiquitin. *Cell* **116**, 181-190 (2004).
726 38. J. Zhang, Q. Liu, Cholesterol metabolism and homeostasis in the brain. *Protein Cell* **6**, 254-264
727 (2015).
728 39. L. Zhang, K. Reue, L. G. Fong, S. G. Young, P. Tontonoz, Feedback regulation of cholesterol uptake
729 by the LXR-IDOL-LDLR axis. *Arterioscler Thromb Vasc Biol* **32**, 2541-2546 (2012).
730 40. J. Gao *et al.*, The E3 ubiquitin ligase IDOL regulates synaptic ApoER2 levels and is important for
731 plasticity and learning. *Elife* **6**, e29178 (2017).
732 41. J. K. Nelson *et al.*, Deubiquitylase Inhibition Reveals Liver X Receptor-independent Transcriptional
733 Regulation of the E3 Ubiquitin Ligase IDOL and Lipoprotein Uptake. *J Biol Chem* **291**, 4813-4825
734 (2016).
735 42. Anonymous, Cytomegalovirus. *Am J Transplant* **4 Suppl 10**, 51-58 (2004).
736 43. Y. Du, G. Zhang, Z. Liu, Human cytomegalovirus infection and coronary heart disease: a systematic
737 review. *Virol J* **15**, 31-31 (2018).
738 44. N. Gudleski-O'Regan, T. M. Greco, I. M. Cristea, T. Shenk, Increased expression of LDL receptor-
739 related protein 1 during human cytomegalovirus infection reduces virion cholesterol and
740 infectivity. *Cell Host Microbe* **12**, 86-96 (2012).
741 45. Y. Xi, S. Harwood, L. M. Wise, J. G. Purdy, Human Cytomegalovirus pUL37x1 Is Important for
742 Remodeling of Host Lipid Metabolism. *J Virol* **93** (2019).
743 46. Y. Xi, L. Lindenmayer, I. Kline, J. von Einem, J. G. Purdy, Human Cytomegalovirus Uses a Host Stress
744 Response To Balance the Elongation of Saturated/Monounsaturated and Polyunsaturated Very-
745 Long-Chain Fatty Acids. *mBio* **12** (2021).
746 47. Y. Yu, T. G. Maguire, J. C. Alwine, Human cytomegalovirus infection induces adipocyte-like
747 lipogenesis through activation of sterol regulatory element binding protein 1. *J Virol* **86**, 2942-
748 2949 (2012).
749 48. Y. Yu, F. J. Pierciey, Jr., T. G. Maguire, J. C. Alwine, PKR-like endoplasmic reticulum kinase is
750 necessary for lipogenic activation during HCMV infection. *PLoS Pathog* **9**, e1003266 (2013).
751 49. D. Collins-McMillen *et al.*, Alternative promoters drive human cytomegalovirus reactivation from
752 latency. *Proceedings of the National Academy of Sciences* **116**, 17492 (2019).
753 50. M.-C. Arcangeletti *et al.*, Human cytomegalovirus reactivation from latency: validation of a
754 "switch" model in vitro. *Virol J* **13**, 179-179 (2016).
755 51. L.-F. Yee, P. L. Lin, M. F. Stinski, Ectopic expression of HCMV IE72 and IE86 proteins is sufficient to
756 induce early gene expression but not production of infectious virus in undifferentiated
757 promonocytic THP-1 cells. *Virology* **363**, 174-188 (2007).

758 52. B. G. Weinshenker, S. Wilton, G. P. Rice, Phorbol ester-induced differentiation permits productive
759 human cytomegalovirus infection in a monocytic cell line. *J Immunol* **140**, 1625-1631 (1988).
760 53. N. Wagenknecht *et al.*, Contribution of the Major ND10 Proteins PML, hDaxx and Sp100 to the
761 Regulation of Human Cytomegalovirus Latency and Lytic Replication in the Monocytic Cell Line
762 THP-1. *Viruses* **7**, 2884-2907 (2015).
763 54. C. H. Lee *et al.*, Factors affecting human cytomegalovirus gene expression in human monocyte cell
764 lines. *Mol Cells* **9**, 37-44 (1999).
765 55. R. N. Ramirez *et al.*, Dynamic Gene Regulatory Networks of Human Myeloid Differentiation. *Cell*
766 *systems* **4**, 416-429.e413 (2017).
767 56. F. O. Martinez, S. Gordon, M. Locati, A. Mantovani, Transcriptional Profiling of the Human
768 Monocyte-to-Macrophage Differentiation and Polarization: New Molecules and Patterns of Gene
769 Expression. *The Journal of Immunology* **177**, 7303 (2006).
770 57. J. D. Horton, J. L. Goldstein, M. S. Brown, SREBPs: activators of the complete program of
771 cholesterol and fatty acid synthesis in the liver. *J Clin Invest* **109**, 1125-1131 (2002).
772 58. J. L. Goldstein, R. A. DeBose-Boyd, M. S. Brown, Protein Sensors for Membrane Sterols. *Cell* **124**,
773 35-46 (2006).
774 59. A. Radhakrishnan, J. L. Goldstein, J. G. McDonald, M. S. Brown, Switch-like control of SREBP-2
775 transport triggered by small changes in ER cholesterol: a delicate balance. *Cell metabolism* **8**, 512-
776 521 (2008).
777 60. S.-Y. Jiang *et al.*, Discovery of a potent HMG-CoA reductase degrader that eliminates statin-
778 induced reductase accumulation and lowers cholesterol. *Nat Commun* **9**, 5138 (2018).
779 61. E. S. Istvan, J. Deisenhofer, Structural Mechanism for Statin Inhibition of HMG-CoA Reductase.
780 **292**, 1160-1164 (2001).
781 62. A. Corsini *et al.*, New insights into the pharmacodynamic and pharmacokinetic properties of
782 statins. *Pharmacology & Therapeutics* **84**, 413-428 (1999).
783 63. K. Warita *et al.*, Statin-induced mevalonate pathway inhibition attenuates the growth of
784 mesenchymal-like cancer cells that lack functional E-cadherin mediated cell cohesion. *Scientific*
785 *Reports* **4**, 7593 (2014).
786 64. P. Gazzerro *et al.*, Pharmacological Actions of Statins: A Critical Appraisal in the Management of
787 Cancer. *Pharmacological Reviews* **64**, 102 (2012).
788 65. A. Koike, K. Tsujinaka, K. Fujimori, Statins attenuate antiviral IFN-β and ISG expression via
789 inhibition of IRF3 and JAK/STAT signaling in poly(I:C)-treated hyperlipidemic mice and
790 macrophages. **288**, 4249-4266 (2021).
791 66. A. Koike, K. Tsujinaka, K. Fujimori, Statins attenuate antiviral IFN-beta and ISG expression via
792 inhibition of IRF3 and JAK/STAT signaling in poly(I:C)-treated hyperlipidemic mice and
793 macrophages. *FEBS J* **288**, 4249-4266 (2021).
794 67. B. P. McSharry *et al.*, Abrogation of the interferon response promotes more efficient human
795 cytomegalovirus replication. *J Virol* **89**, 1479-1483 (2015).
796 68. C. M. Goodwin, J. H. Ciesla, J. Munger, Who's Driving? Human Cytomegalovirus, Interferon, and
797 NFκB Signaling. *Viruses* **10** (2018).
798 69. V. R. DeFilippis, D. Alvarado, T. Sali, S. Rothenburg, K. Früh, Human Cytomegalovirus Induces the
799 Interferon Response via the DNA Sensor ZBP1. **84**, 585-598 (2010).
800 70. B. Göker Bağca, C. J. F. Avci, B. T. Dergisi, Ruxolitinib and effect mechanisms. **2**, 153-157 (2016).
801 71. S. D. Lee, P. Tontonoz, Liver X receptors at the intersection of lipid metabolism and atherogenesis.
802 *Atherosclerosis* **242**, 29-36 (2015).
803 72. B. A. Janowski *et al.*, Structural requirements of ligands for the oxysterol liver X receptors LXRalpha
804 and LXRbeta. *Proc Natl Acad Sci U S A* **96**, 266-271 (1999).

805 73. B. A. Janowski, P. J. Willy, T. R. Devi, J. R. Falck, D. J. Mangelsdorf, An oxysterol signalling pathway
806 mediated by the nuclear receptor LXRα. *Nature* **383**, 728-731 (1996).
807 74. D. J. Peet, B. A. Janowski, D. J. Mangelsdorf, The LXRs: a new class of oxysterol receptors. *Current*
808 *Opinion in Genetics & Development* **8**, 571-575 (1998).
809 75. A. C. Calkin *et al.*, FERM-dependent E3 ligase recognition is a conserved mechanism for targeted
810 degradation of lipoprotein receptors. **108**, 20107-20112 (2011).
811 76. B. Liu *et al.*, Inhibition of Human Cytomegalovirus Particle Maturation by Activation of Liver X
812 Receptor. *Front Microbiol* **13**, 846386-846386 (2022).
813 77. Q. Wang *et al.*, Identification of interferon-γ as a new molecular target of liver X receptor.
814 *Biochemical Journal* **459**, 345-354 (2014).
815 78. B. Sainz, H. L. LaMarca, R. F. Garry, C. A. Morris, Synergistic inhibition of human cytomegalovirus
816 replication by interferon-alpha/beta and interferon-gamma. *Virol J* **2**, 14 (2005).
817 79. K. A. Kropp *et al.*, Reversible inhibition of murine cytomegalovirus replication by gamma
818 interferon (IFN-γ) in primary macrophages involves a primed type I IFN-signaling subnetwork for
819 full establishment of an immediate-early antiviral state. *Journal of virology* **85**, 10286-10299
820 (2011).
821 80. L. Fagerberg *et al.*, Analysis of the human tissue-specific expression by genome-wide integration
822 of transcriptomics and antibody-based proteomics. *Molecular & cellular proteomics : MCP* **13**,
823 397-406 (2014).
824 81. I. Fernandez-Ruiz, P. Puchalska, C. A. Narasimhulu, B. Sengupta, S. Parthasarathy, Differential lipid
825 metabolism in monocytes and macrophages: influence of cholesterol loading[S]. *Journal of Lipid*
826 *Research* **57**, 574-586 (2016).
827 82. T. R. Cimato, B. A. Palka, J. K. Lang, R. F. Young, LDL Cholesterol Modulates Human CD34+ HSPCs
828 through Effects on Proliferation and the IL-17 G-CSF Axis. *PLOS ONE* **8**, e73861 (2013).
829 83. P. K. Morgan, L. Fang, G. I. Lancaster, A. J. Murphy, Hematopoiesis is regulated by cholesterol
830 efflux pathways and lipid rafts: connections with cardiovascular diseases: Thematic Review Series:
831 Biology of Lipid Rafts. *Journal of Lipid Research* **61**, 667-675 (2020).
832 84. O. Soehnlein, F. K. Swirski, Hypercholesterolemia links hematopoiesis with atherosclerosis. *Trends*
833 *in endocrinology and metabolism: TEM* **24**, 129-136 (2013).
834 85. Y. Wang *et al.*, Pseudorabies Virus Inhibits Expression of Liver X Receptors to Assist Viral Infection.
835 *Viruses* **14**, 514 (2022).
836 86. P. T. Lange, C. Schorl, D. Sahoo, V. L. Tarakanova, Liver X Receptors Suppress Activity of Cholesterol
837 and Fatty Acid Synthesis Pathways To Oppose Gammaherpesvirus Replication. *mBio* **9**, e01115-
838 01118 (2018).
839 87. P. T. Lange, C. N. Jondle, E. J. Darrah, K. E. Johnson, V. L. Tarakanova, LXR Alpha Restricts
840 Gammaherpesvirus Reactivation from Latently Infected Peritoneal Cells. *Journal of virology* **93**,
841 e02071-02018 (2019).
842 88. J. Zeng *et al.*, Liver X receptors agonists impede hepatitis C virus infection in an Idol-dependent
843 manner. *Antiviral Res* **95**, 245-256 (2012).
844 89. S. Bocchetta *et al.*, Up-regulation of the ATP-binding cassette transporter A1 inhibits hepatitis C
845 virus infection. *PLoS One* **9**, e92140 (2014).
846 90. H. Jiang *et al.*, Retinoic acid and liver X receptor agonist synergistically inhibit HIV infection in CD4+
847 T cells by up-regulating ABCA1-mediated cholesterol efflux. *Lipids Health Dis* **11**, 69 (2012).
848 91. L. Dubrovsky *et al.*, Liver X receptor agonist inhibits HIV-1 replication and prevents HIV-induced
849 reduction of plasma HDL in humanized mouse model of HIV infection. *Biochem Biophys Res*
850 *Commun* **419**, 95-98 (2012).
851 92. T. M. Hanley, G. A. Viglianti, Nuclear receptor signaling inhibits HIV-1 replication in macrophages
852 through multiple trans-repression mechanisms. *J Virol* **85**, 10834-10850 (2011).

853 93. X. X. Sheng *et al.*, The LXR ligand GW3965 inhibits Newcastle disease virus infection by affecting
854 cholesterol homeostasis. *Arch Virol* **161**, 2491-2501 (2016).
855 94. J. Zeng *et al.*, Liver X receptors agonists impede hepatitis C virus infection in an Idol-dependent
856 manner. *Antiviral Research* **95**, 245-256 (2012).
857 95. G. H. Syed *et al.*, Hepatitis C virus stimulates low-density lipoprotein receptor expression to
858 facilitate viral propagation. *Journal of virology* **88**, 2519-2529 (2014).
859 96. A. Albecka *et al.*, Role of low-density lipoprotein receptor in the hepatitis C virus life cycle.
860 *Hepatology (Baltimore, Md.)* **55**, 998-1007 (2012).
861 97. S. Molina *et al.*, The low-density lipoprotein receptor plays a role in the infection of primary
862 human hepatocytes by hepatitis C virus. *Journal of hepatology* **46**, 411-419 (2007).
863 98. B. Sun *et al.*, Regulation of host and virus genes by neuronal miR-138 favours herpes simplex virus
864 1 latency. *Nature microbiology* **6**, 682-696 (2021).
865 99. D. Pan *et al.*, A neuron-specific host microRNA targets herpes simplex virus-1 ICP0 expression and
866 promotes latency. *Cell Host Microbe* **15**, 446-456 (2014).
867 100. X. Liu *et al.*, Herpesvirus-mediated stabilization of ICP0 expression neutralizes restriction by
868 TRIM23. *Proc Natl Acad Sci U S A* **118** (2021).
869 101. T. H. Chang *et al.*, Regulation of the Abundance of Kaposi's Sarcoma-Associated Herpesvirus
870 ORF50 Protein by Oncoprotein MDM2. *PLoS Pathog* **12**, e1005918 (2016).
871 102. J. C. Chmura *et al.*, The Itch ubiquitin ligase is required for KSHV RTA induced vFLIP degradation.
872 *Virology* **501**, 119-126 (2017).
873 103. E. S. Ehrlich, J. C. Chmura, J. C. Smith, N. N. Kalu, G. S. Hayward, KSHV RTA abolishes NFkappaB
874 responsive gene expression during lytic reactivation by targeting vFLIP for degradation via the
875 proteasome. *PLoS One* **9**, e91359 (2014).
876 104. S. Gandon, Why Be Temperate: Lessons from Bacteriophage λ. *Trends in Microbiology* **24**, 356-
877 365 (2016).
878 105. S. Atsumi, J. W. Little, Role of the lytic repressor in prophage induction of phage lambda as
879 analyzed by a module-replacement approach. *Proceedings of the National Academy of Sciences*
880 *of the United States of America* **103**, 4558-4563 (2006).
881 106. R. A. Schubert, I. B. Dodd, J. B. Egan, K. E. Shearwin, Cro's role in the CI Cro bistable switch is critical
882 for {lambda}'s transition from lysogeny to lytic development. *Genes Dev* **21**, 2461-2472 (2007).
883 107. M. G. Cortes, J. T. Trinh, L. Zeng, G. Balazsi, Late-Arriving Signals Contribute Less to Cell-Fate
884 Decisions. *Biophys J* **113**, 2110-2120 (2017).
885 108. O. Kobiler, A. Rokney, A. B. Oppenheim, Phage lambda CIII: a protease inhibitor regulating the
886 lysis-lysogeny decision. *PLoS One* **2**, e363 (2007).
887 109. J. W. Little, D. P. Shepley, D. W. J. T. E. j. Wert, Robustness of a gene regulatory circuit. **18**, 4299-
888 4307 (1999).
889 110. J. D. Hernandez-Doria, V. Sperandio, Bacteriophage Transcription Factor Cro Regulates Virulence
890 Gene Expression in Enterohemorrhagic Escherichia coli. *Cell Host Microbe* **23**, 607-617.e606
891 (2018).
892 111. M. Peppenelli, J. Buehler, F. Goodrum, Human Hematopoietic Long-Term Culture (hLTC) for
893 Human Cytomegalovirus Latency and Reactivation. *Methods Mol Biol* **2244**, 83-101 (2021).
894 112. M. Umashankar *et al.*, A Novel Human Cytomegalovirus Locus Modulates Cell Type-Specific
895 Outcomes of Infection. *PLOS Pathogens* **7**, e1002444 (2011).
896 113. N. E. Sanjana, O. Shalem, F. Zhang, Improved vectors and genome-wide libraries for CRISPR
897 screening. *Nat Methods* **11**, 783-784 (2014).

898

899

900 **Figure legends**

901

902 **Figure 1. UL136p33 isoform is rapidly turned over by the proteasome.** (A) Schematic
903 depiction of the *UL133-UL138* polycistronic gene locus and UL136 protein isoforms. A C-
904 terminal myc tag is used to detect UL136 isoforms. Red lines represent lysine residues,
905 and the black box shows the putative transmembrane domain. (B-D) Fibroblasts were
906 infected with TB40/E-$UL136_{myc}$ virus at a MOI of 1. (B) At 48 hpi, cells were treated with
907 50 µg/ml cycloheximide (CHX) for 6 h. Alternatively, mock- or TB40/E-infected cells were
908 treated with CHX in the context of proteasomal (MG132) or lysosomal (NH_4Cl) inhibition
909 (right panel). $UL136_{myc}$ protein isoforms or tubulin as a loading control were detected by
910 immunoblotting using by a monoclonal α-myc antibody or tubulin, respectively (left panel).
911 (C) Cells were untreated or treated with CHX at 48 hpi and UL136 decay was analyzed
912 over a 6-hour time course by immunoblotting. (D) Relative quantification of UL136
913 isoforms normalized to tubulin.

914

915 **Figure 2. Stabilizing UL136p33 results in virus that fails to establish latency.** (A)
916 Fibroblasts were transduced with lentiviruses engineered to express $p33_{myc}$ or $p33_{K\rightarrow R}$
917 and protein decay was analyzed by immunoblotting following CHX treatment. (B)
918 Fibroblasts were infected with TB40/E-$UL136_{myc}$ or -$UL136_{myc}\Delta K\rightarrow R$ viruses (MOI =1)
919 and treated with CHX at 48 hpi or left untreated. Protein decay was analyzed as described
920 in Figure 1C. (C) Fibroblasts were infected at a MOI of 0.02 and samples collected for
921 $TCID_{50}$ at indicated times. All data points are an average of 3 biological replicates and
922 error bars represent standard deviation. (D) CD34+ HPCs were infected with $UL136_{myc}$
923 or $UL136_{myc}\Delta K\rightarrow R$ viruses (MOI=2). Infected cells were purified by FACS at 1 dpi seeded

924 into long term culture. At 10 days, half of the culture was reactivated by seeding intact
925 cells by limiting dilution into co-culture with fibroblasts in a cytokine-rich media to promote
926 myeloid differentiation (reactivation). The other half of the culture was mechanically lysed
927 and seeded onto fibroblasts as the pre-reactivation control. The frequency of infectious
928 centers was determined for each sample by extreme limiting dilution. (C-D) The data
929 represents replicates with cells from 3 independent donors. The means were compared
930 with two-way analysis of variance (ANOVA) with a Tukey post hoc test and the were no
931 significant differences. **, $p<0.01$; ***, $p<0.001$.
932
933 **Figure 3. The host E3 ligase IDOL specifically targets UL136p33 for turnover.** (A)
934 HEK cells were transiently transfected with plasmids expressing UL136p33, IDOL, empty
935 vector, or the indicated combinations. UL136p33 or IDOL was immunoprecipitated from
936 protein lysates using α-myc or α-HA magnetic beads. Protein was detected by
937 immunoblotting using the antibodies indicated. Lysates were blotted as a control for
938 expression and GAPDH used as a loading control. (B) HEK cells were transiently
939 transfected with plasmids expressing $p33_{\Delta K \rightarrow R}$, IDOL, or empty vector. Proteins were
940 detected by immunoblotting using α-myc or α-HA monoclonal antibodies. (C) Protein
941 densities of UL136p33 (from panel A) or $p33_{\Delta K \rightarrow R}$ (from panel B) relative to their loading
942 control. (D) HEK cells were transiently transfected to express UL136p33 or $p33_{\Delta K \rightarrow R.}$ IDOL
943 was induced 48 hours later with 2 μM of LXR-agonists, GW3965 or HBX41-108, or vehicle
944 (DMSO) for 6 h. Detection of ApoER-2 was used as a proxy for validating the induction
945 of IDOL. $p33_{myc}$, $p33_{K \rightarrow R}$, and tubulin as a loading control were detected by
946 immunoblotting using α-myc or α-tubulin. All data points represent the mean of at least 3

947 independent replicates and the means were compared by two-way ANOVA with a Tukey
948 post hoc test. Error bars represent standard deviation. ns, $p>0.05$. ****, $p<0.0001$.
949
950 **Figure 4. Induction of IDOL in CD34+ HPCs inhibits reactivation.** (A) CD34+ HPCs
951 were mock- or TB40/E-infected at a MOI of 2. At 1 dpi, cells were treated with 1 μM
952 GW3965 for 6 h and total RNA isolated for qPCR to measure *IDOL* transcript levels
953 relative to *H6PD*. The data points represent the mean from 3 independent experiments.
954 The means were analyzed by two-way ANOVA with a Tukey post-hoc test. ***$p<0.001$;
955 ****, $p<0.0001$. (B) CD34+ HPCs were infected at a MOI of 2. At 24 hpi, infected CD34+
956 cells were isolated by FACS and seeded into long term culture. At 10 days, half of the
957 culture was reactivated by seeding intact cells by limiting dilution into co-culture with
958 fibroblasts in a cytokine-rich media to promote myeloid differentiation (reactivation). The
959 other half of the culture was mechanically lysed and seeded onto fibroblasts as the pre-
960 reactivation control. The frequency of infectious centers was determined for each sample
961 by ELDA. The data points represent replicates from 2 independent donors and the range
962 is indicated by squares (pre-reactivation) and dots (post-reactivation).
963
964 **Figure 5. IDOL impacts viral protein expression in a THP-1 cell latency model.** (A)
965 Total RNA was extracted from mock-, $UL136_{myc}$- or $UL136_{myc}\Delta K\rightarrow R$-infected THP-1 cells
966 at indicated time points. At 5 dpi, cells were treated with TPA to induce differentiation or
967 the vehicle control (DMSO). cDNA was synthesized from the RNA and qPCR was used
968 to determine the relative expression levels of *IDOL* transcripts compared to the low copy
969 cellular housekeeping gene *H6PD* using the ΔΔCT method. (B) Validation of *IDOL* KO in

970 undifferentiated THP-1 cells was confirmed by ELISA. Where indicated, cells were treated
971 with TPA as a positive control for the loss of IDOL. (C) Immunoblot of HDAC1 in *Luc*
972 control or *IDOL* KO THP-1 cells to rule out off-target CRISPR/CAS9 effects. (D) *IDOL* or
973 *Luc* KO THP-1 cells were infected with TB40/E-*UL136*$_{myc}$ (top panel) or -*UL136*$_{myc}$*K→R*
974 (bottom panel) at a MOI of 2 and cell lysates were collected at indicated time points. IE1/2
975 and UL135 accumulation was evaluated by immunoblotting protein lysates over a time
976 course using a monoclonal α-IE1/2 and polyclonal α-UL135. (E) IE1/2 and UL135 were
977 quantified, and levels normalized to Tubulin and levels present at 1 dpi in the Luc KO
978 control. All data points are representative of the mean 3 independent replicates and error
979 bars represent standard deviation. The means were compared by two-way ANOVA with
980 a Tukey post hoc test. ns, $p>0.05$; *, $p<0.05$; **, $p<0.01$; ****, $p<0.0001$.
981
982 **Figure 6. *de novo* cholesterol biosynthesis is required for reactivation from latency.**
983 (A) THP-1 cells were mock- or HCMV-infected at a MOI of 2 and total cholesterol was
984 measured at indicated times. (B) Total RNA was extracted from THP-1 cells to validate
985 pravastatin (PRV)-mediated inhibition of HMGCR as measured by *SREBP2* transcripts.
986 (C) Relative IE1 and IE2 transcripts were measured in infected THP-1 cells by qPCR at
987 2 days post differentiation following treatments with TPA, TPA and PRV, or TPA with PRV
988 and mevalonate (MEV). IE transcripts were normalized to *H6PD* transcripts. (D) *IFN-β1*
989 transcripts were measured by qPCR in the context of treatment with TPA, TPA with PRV,
990 or TPA with PRV and MEV. (E) Cell lysates were obtained from infected cells in which
991 ruxolitinib was used to block JAK/STAT signaling. pSTAT1 level in TPA-treated cells were
992 used as baseline control. (F) RT-qPCR analysis of IE1 and IE2 expression when IFN

993 signaling was disrupted by the JAK/STAT inhibitor ruxolitinib in the context of PRV and
994 MEV treatment, as indicated. All data points are representative of the mean 3
995 independent replicates and error bars represent standard deviation. The means were
996 compared by two-way ANOVA with a Tukey post hoc test. ns, $p>0.05$; *, $p<0.05$; **,
997 $p<0.01$; ****, $p<0.0001$.
998
999 **Figure 7. Model for differentiation-dependent IDOL regulation to control UL136p33**
1000 **levels.** Progenitor cells are relatively small and are intolerant of high cholesterol, which
1001 they control by upregulating IDOL. We propose that high levels of IDOL maintain low
1002 levels of UL136p33 for the establishment of latency. Upon cell differentiation, cells
1003 downregulate IDOL, which would result in a corresponding increase in UL136p33 levels
1004 to drive infection towards reactivation. UL136p33 levels are further increased upon the
1005 commitment to viral DNA synthesis. Stabilization of UL136p33 results in corresponding
1006 downregulation of IDOL mRNAs, suggesting feedback to suppress of IDOL gene
1007 expression. This work implicates IDOL as a host factor that fine-tunes levels of UL136p33
1008 to control decisions to enter and exit latency. These findings further indicate a key role for
1009 cholesterol homeostasis as a determinant of HCMV reactivation, whereby UL136p33 acts
1010 as a sensor at the tipping point between the decision to maintain the latent state or exit
1011 latency for reactivation. Cholesterol represented by beige droplets. Figure made with
1012 Biorender.com.

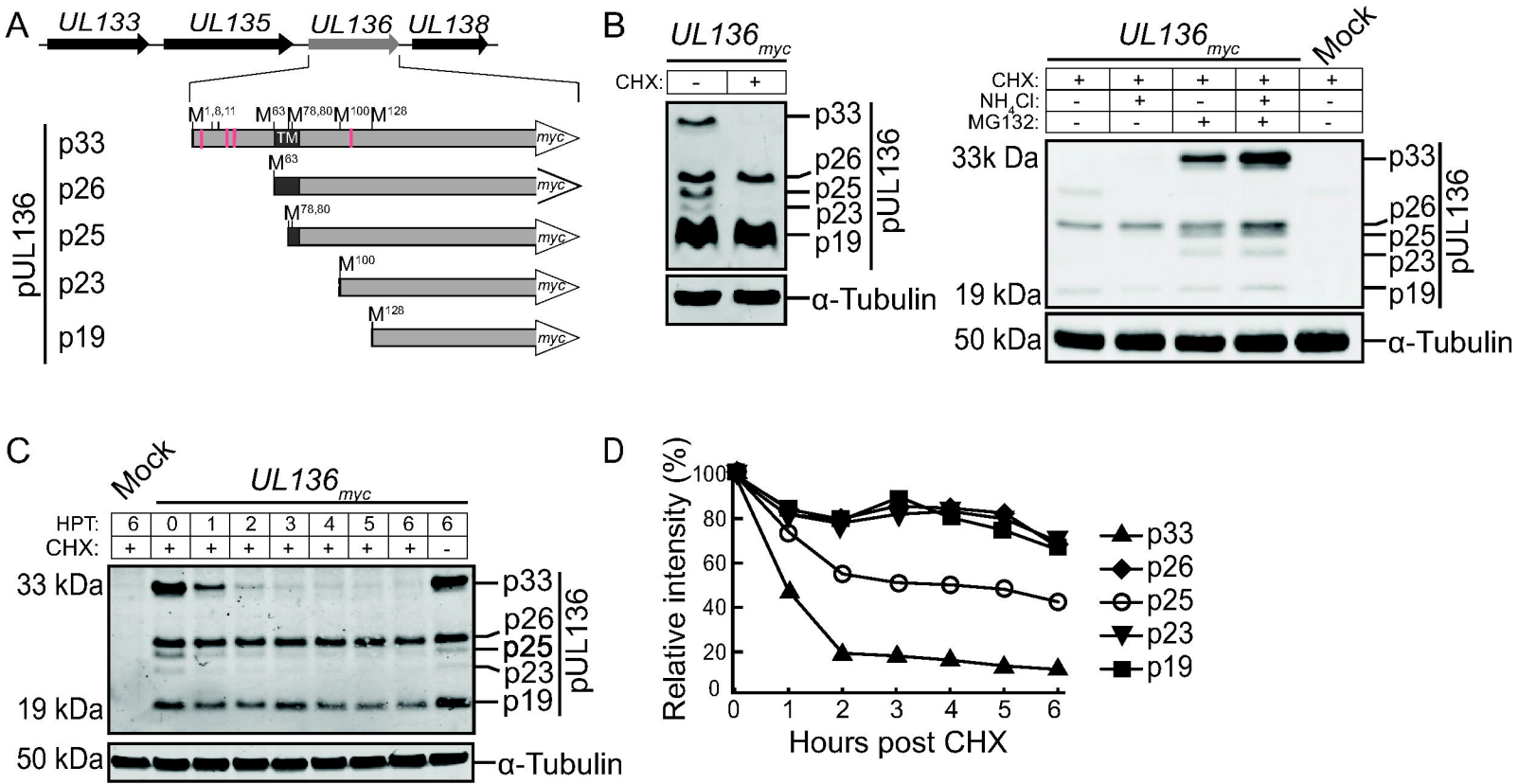
A
UL133
UL135
UL136
UL138
M1,8,11
M63
M78,80
M100
M128
TM
myc
pUL136
p33
p26
p25
p23
p19
B
UL136myc
CHX:
-
+
p33
p26
p25
p23
p19
pUL136
α-Tubulin
Mock
NH4Cl:
MG132:
33k Da
19 kDa
50 kDa
C
HPT:
6
0
1
2
3
4
5
6
33 kDa
19 kDa
50 kDa
D
Relative intensity (%)
Hours post CHX
100
80
60
40
20
0
0
1
2
3
4
5
6

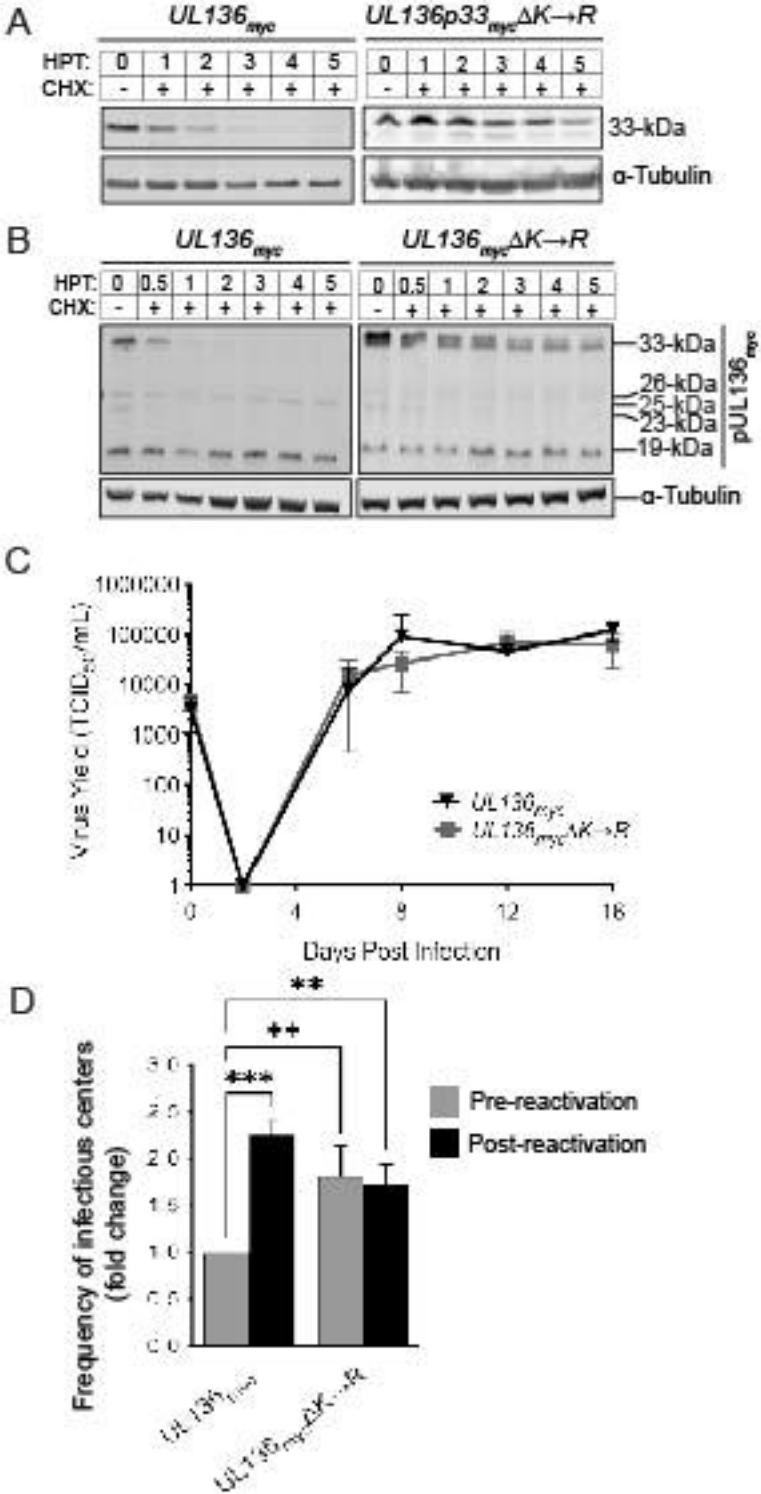
A
UL136myc
UL136p33mycΔK→R
HPT: 0 1 2 3 4 5
CHX: - + + + + +
33-kDa
α-Tubulin
B
UL136myc
UL136mycΔK→R
HPT: 0 0.5 1 2 3 4 5
CHX: - + + + + +
33-kDa
26-kDa
25-kDa
23-kDa
19-kDa
pUL136myc
α-Tubulin
C
Virus Yield (TCID50/mL)
1000000
100000
10000
1000
100
10
1
0
4
8
12
16
Days Post Infection
UL136myc
UL136mycΔK→R
D
Frequency of infectious centers (fold change)
3.0
2.5
2.0
1.5
1.0
0.5
0.0
***
**
**
Pre-reactivation
Post-reactivation
UL136myc
UL136mycΔK→R

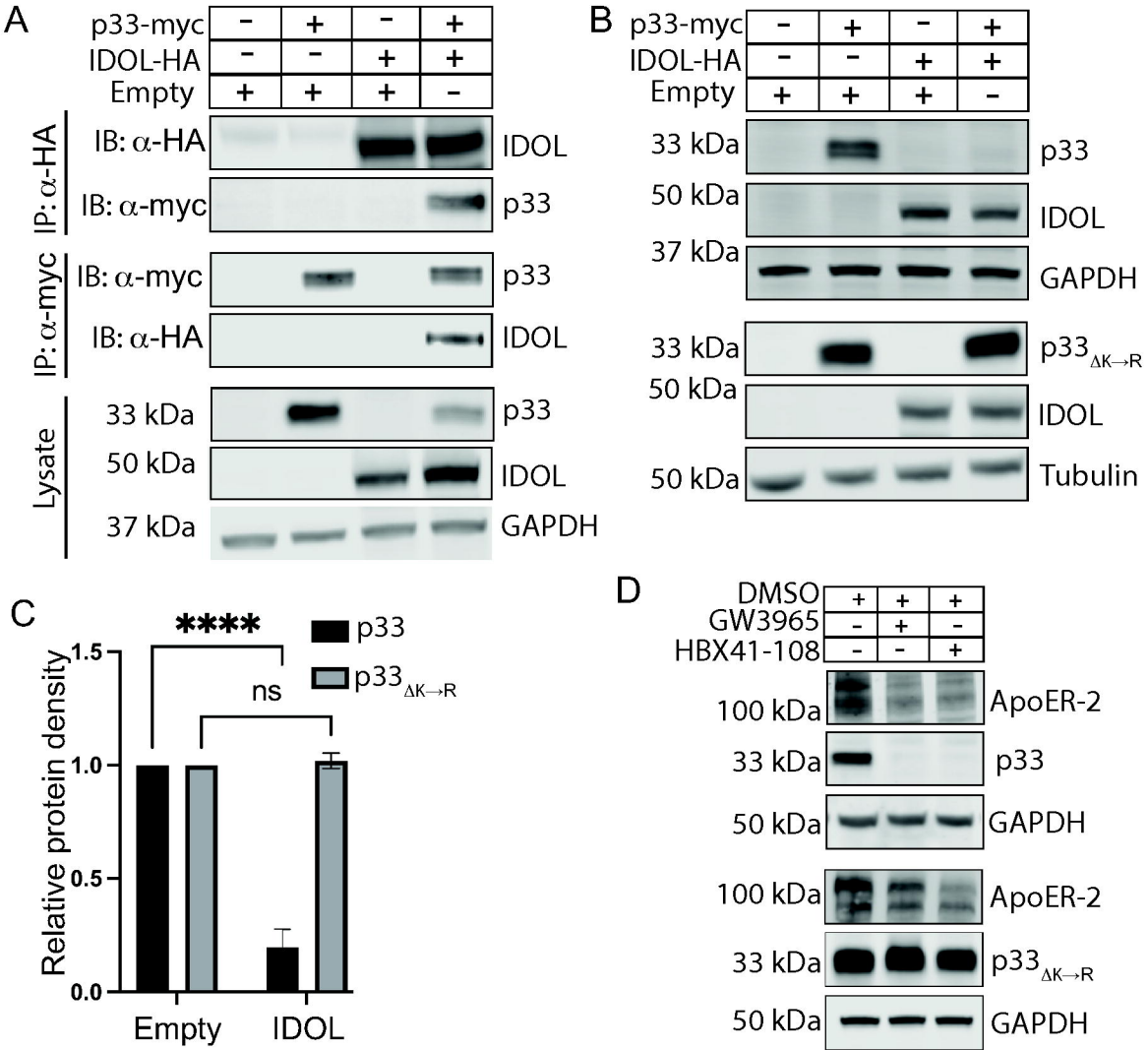
A
p33-myc
IDOL-HA
Empty
IP: α-HA
IB: α-HA
IDOL
IB: α-myc
p33
IP: α-myc
IB: α-myc
p33
IB: α-HA
IDOL
Lysate
33 kDa
p33
50 kDa
IDOL
37 kDa
GAPDH
B
p33-myc
IDOL-HA
Empty
33 kDa
p33
50 kDa
IDOL
37 kDa
GAPDH
33 kDa
p33ΔK→R
50 kDa
IDOL
50 kDa
Tubulin
C
****
ns
p33
p33ΔK→R
Relative protein density
1.5
1.0
0.5
0.0
Empty
IDOL
D
DMSO
GW3965
HBX41-108
100 kDa
ApoER-2
33 kDa
p33
50 kDa
GAPDH
100 kDa
ApoER-2
33 kDa
p33ΔK→R
50 kDa
GAPDH

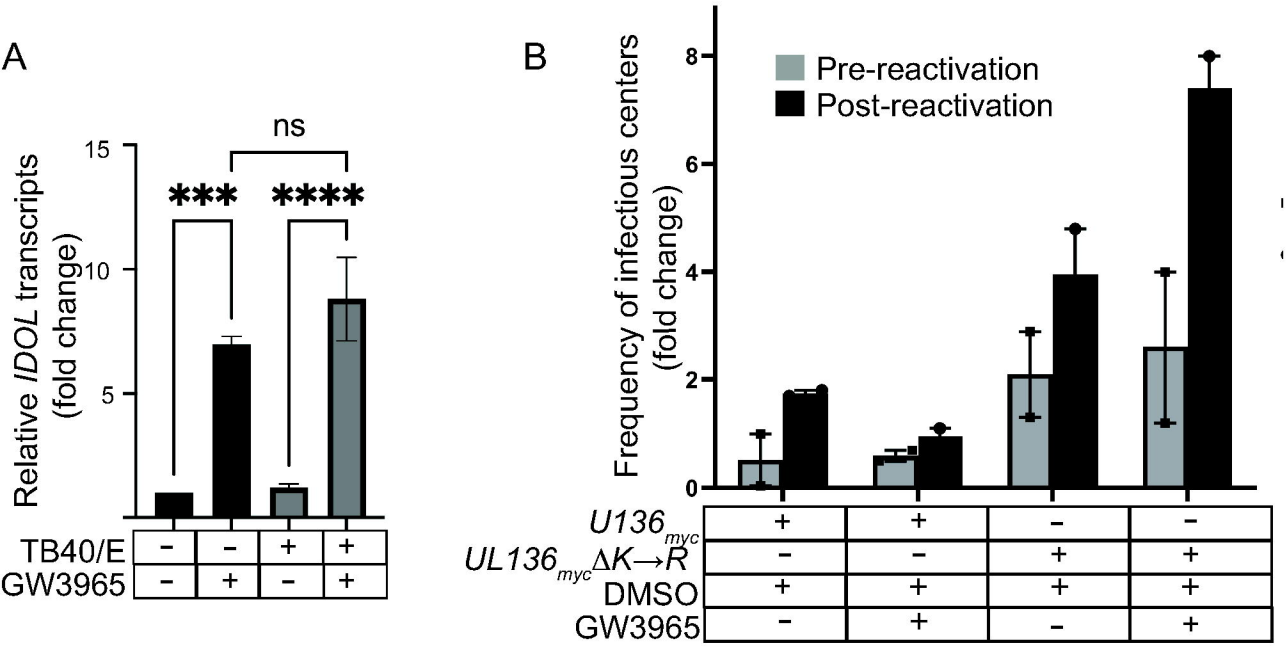
A
ns
***
****
15
10
5
Relative IDOL transcripts
(fold change)
TB40/E
GW3965
B
Pre-reactivation
Post-reactivation
8
6
4
2
0
Frequency of infectious centers
(fold change)
U136myc
UL136myc ΔK→R
DMSO
GW3965

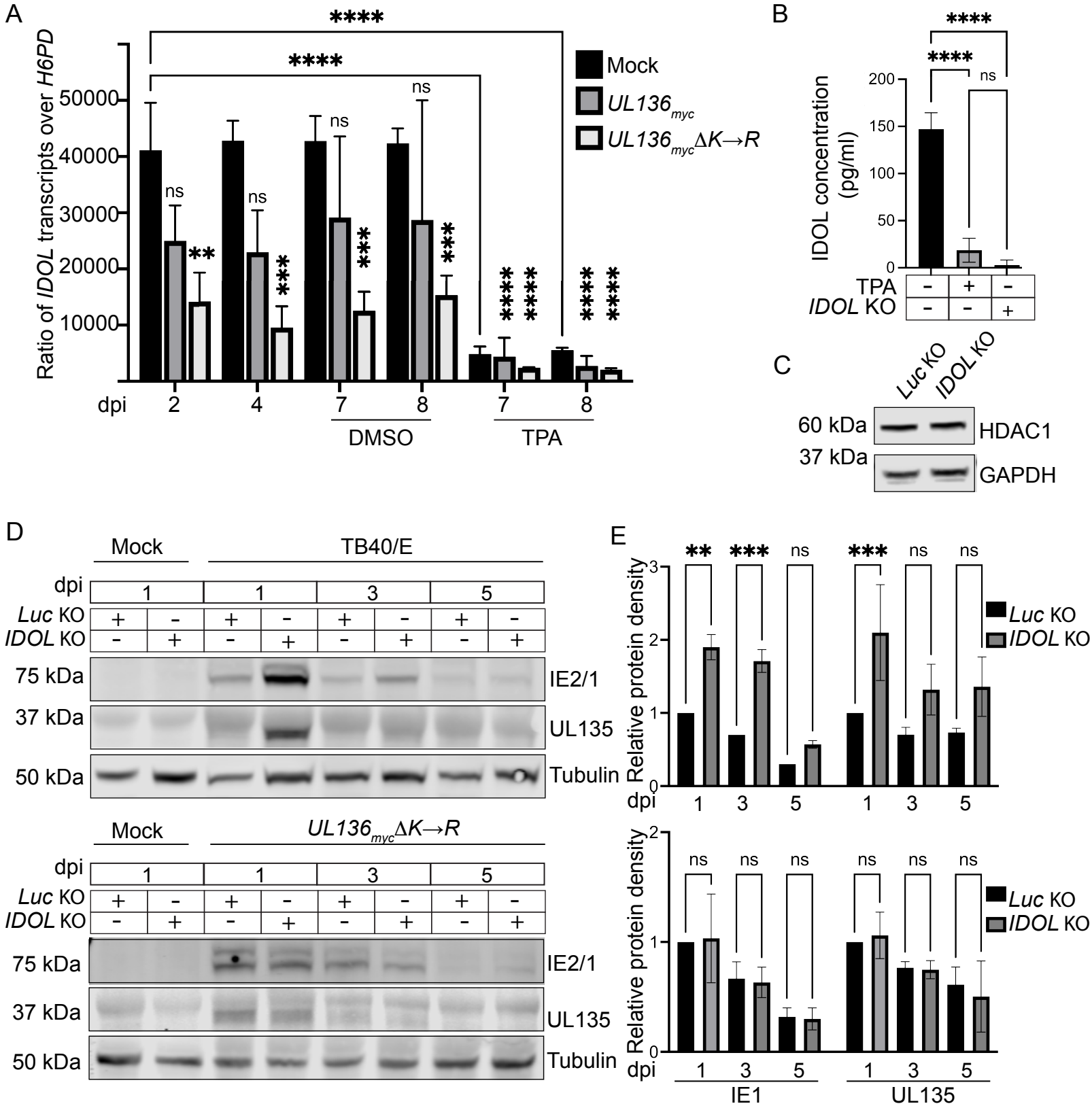
A
Ratio of IDOL transcripts over H6PD
50000
40000
30000
20000
10000
****
****
ns
**
***
Mock
UL136myc
UL136mycΔK→R
dpi
2
4
7
8
7
8
DMSO
TPA
B
IDOL concentration (pg/ml)
200
150
100
50
0
TPA
IDOL KO
C
Luc KO
IDOL KO
60 kDa
HDAC1
37 kDa
GAPDH
D
Mock
TB40/E
dpi
Luc KO
IDOL KO
75 kDa
IE2/1
37 kDa
UL135
50 kDa
Tubulin
UL136mycΔK→R
E
Relative protein density
Luc KO
IDOL KO
IE1
UL135

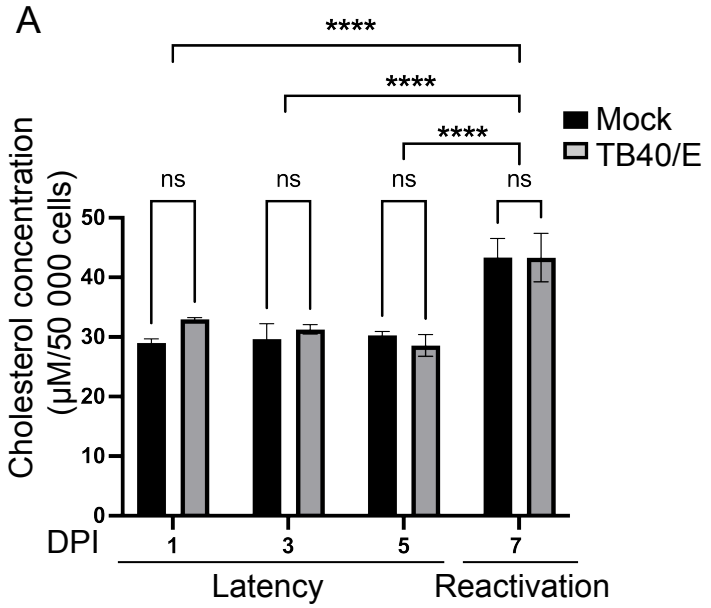
A
Cholesterol concentration (µM/50 000 cells)
Mock
TB40/E
ns
****
DPI
1
3
5
7
Latency
Reactivation

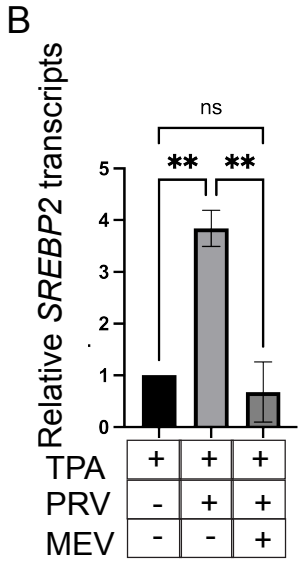
B
Relative SREBP2 transcripts
ns
**
TPA
PRV
MEV

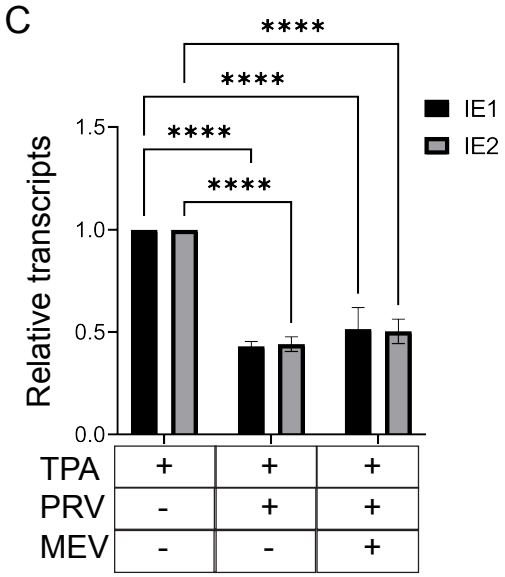
C
Relative transcripts
IE1
IE2
****
TPA
PRV
MEV

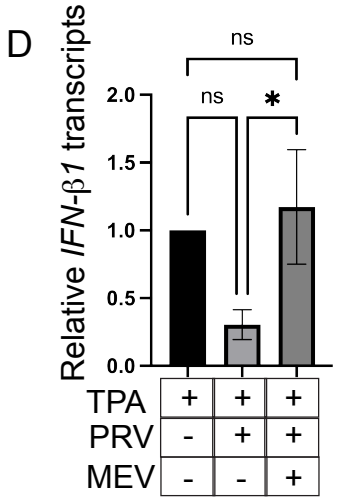
D
Relative IFN-β1 transcripts
ns
*
TPA
PRV
MEV

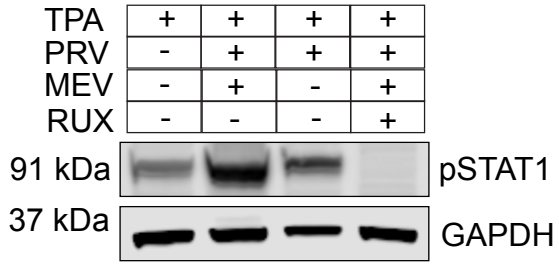
E
TPA
PRV
MEV
RUX
91 kDa
pSTAT1
37 kDa
GAPDH

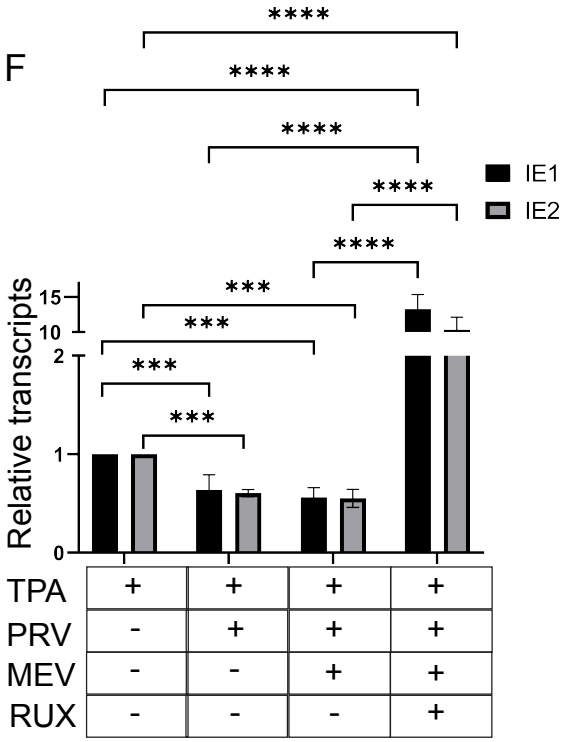
F
Relative transcripts
IE1
IE2
****
***
TPA
PRV
MEV
RUX

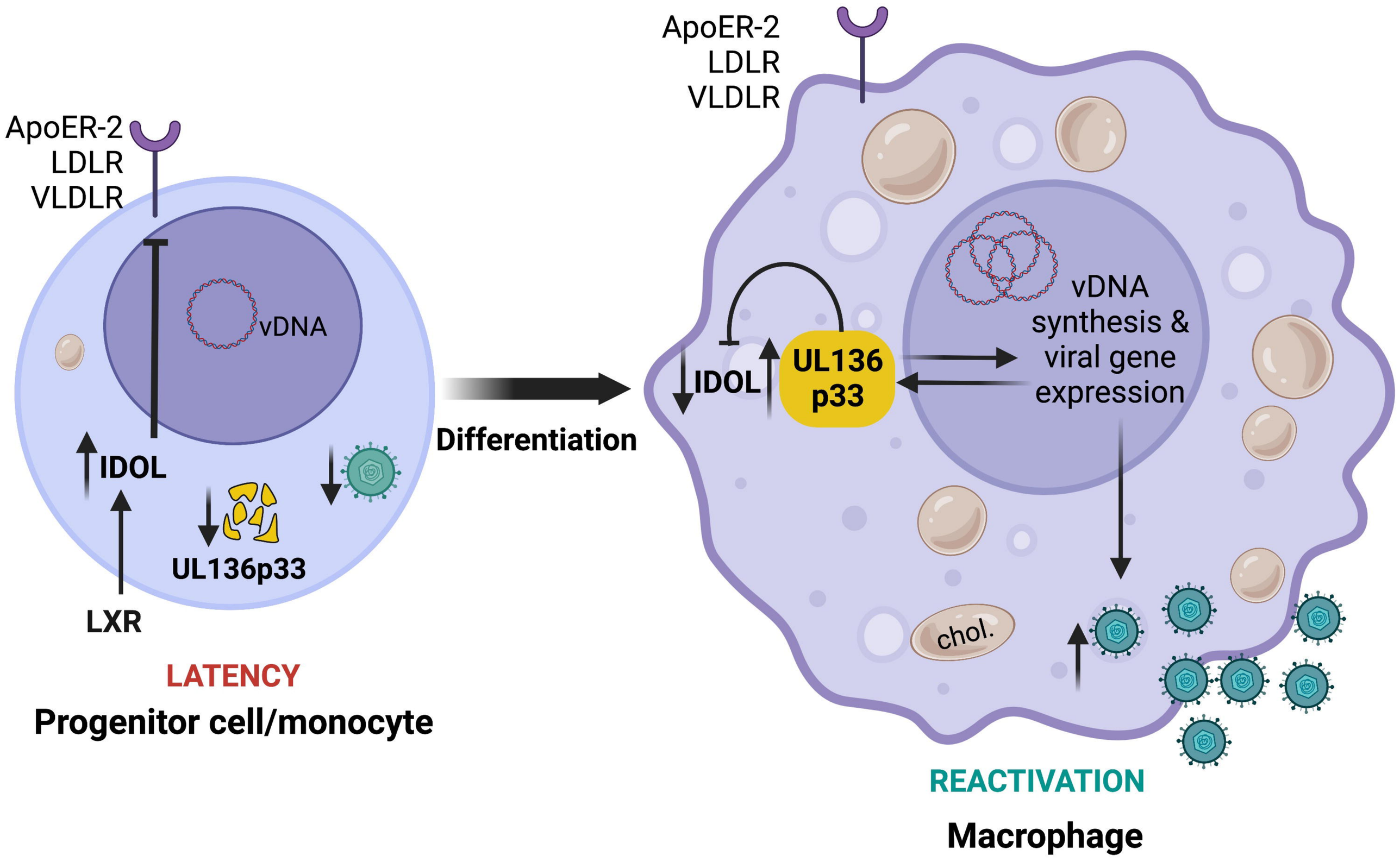
ApoER-2
LDLR
VLDLR
vDNA
IDOL
UL136p33
LXR
LATENCY
Progenitor cell/monocyte
Differentiation
ApoER-2
LDLR
VLDLR
IDOL
UL136
p33
vDNA
synthesis &
viral gene
expression
chol.
REACTIVATION
Macrophage